Eur. Phys. J. C 40, 395–417 (2005)
Digital Object Identifier (DOI) 10.1140/epjc/s2005-02147-7

THE EUROPEAN PHYSICAL JOURNAL C

Two-parton twist-3 factorization in perturbative QCD

Makiko Nagashima[1,a], Hsiang-nan Li[2,3]

[1] Department of Physics, Ochanomizu University, Bunkyo-ku, Tokyo 112-8610, Japan
[2] Institute of Physics, Academia Sinica, Taipei, Taiwan 115, Republic of China
[3] Department of Physics, National Cheng-Kung University, Tainan, Taiwan 701, Republic of China

Received: 8 June 2004 / Revised version: 10 December 2004 /
Published online: 3 March 2005 –

Abstract. We prove the collinear factorization theorem for the process $\pi\gamma^* \to \pi$ at the twist-3 level in the covariant gauge by means of the Ward identity, concentrating on the two-parton case. It is shown that soft divergences cancel and collinear divergences are grouped into the pseudo-scalar and pseudo-tensor two-parton twist-3 pion distribution amplitudes. The delicate summation of a complete set of diagrams for achieving factorization in momentum, spin, and color spaces is emphasized. The proof is then extended to the exclusive semileptonic decay $B \to \pi l\nu$, assuming the hard scale to be of $O(\sqrt{\bar{\Lambda} M_B})$, where $\bar{\Lambda}$ is a hadronic scale and M_B the B meson mass. We explain the distinction between the factorization of collinear divergences for a pion distribution amplitude and of soft divergences for a B meson distribution amplitude. The gauge invariance and universality of the two-parton twist-3 pion distribution amplitudes are confirmed. The proof presented here can accommodate the leading twist-2 case. We then compare our proof with that performed in the framework of soft-collinear effective theory.

PACS. 12.38.Bx

1 Introduction

Recently, we have proposed a simple proof of the collinear factorization theorem in perturbative QCD (PQCD) for the exclusive processes $\pi\gamma^* \to \gamma(\pi)$ and $B \to \gamma(\pi) l\bar{\nu}$ based on the Ward identity [1]. According to this theorem [2–6], hadronic form factors are factorized into the convolution of hard amplitudes with hadron distribution amplitudes in momentum, spin, and color spaces. The former, being infrared finite, are calculable in perturbation theory. The latter, absorbing the infrared divergences involved in the processes, are defined as matrix elements of non-local operators. The universality of the distribution amplitudes and the gauge invariance of the factorization have been explicitly demonstrated. Our proof can be compared to that performed in the axial gauge [2], in which the factorization of infrared divergences is trivial, but the gauge invariance is not obvious. The formalism in [1] is restricted to the leading-twist, i.e., twist-2 level. As emphasized in [7, 8], contributions from the two-parton twist-3 pion distribution amplitudes are not only chirally enhanced, but are of the same power as the leading-twist one in the semileptonic decay $B \to \pi l\nu$. Hence, it is necessary to derive the corresponding factorization theorem. This proof can be regarded as an essential step toward a rigorous construction of the factorization theorem for two-body non-leptonic B meson decays.

[a] e-mail: makiko@phys.ntu.edu.tw

The general decompositions of the matrix elements relevant to the two-parton pion distribution amplitudes are [9]

$$\langle 0|\bar{d}(y)\gamma_\mu\gamma_5 u(0)|\pi^+(P)\rangle = \mathrm{i} f_\pi P_\mu \int_0^1 \mathrm{d}x \mathrm{e}^{-\mathrm{i}xP\cdot y}\phi_P(x) + \frac{\mathrm{i}}{2} f_\pi M_\pi^2 \frac{y_\mu}{P\cdot y}\int_0^1 \mathrm{d}x \mathrm{e}^{-\mathrm{i}xP\cdot y} g_\pi(x)\,, \tag{1}$$

$$\langle 0|\bar{d}(y)\gamma_5 u(0)|\pi^+(P)\rangle = -\mathrm{i} f_\pi m_0 \int_0^1 \mathrm{d}x \mathrm{e}^{-\mathrm{i}xP\cdot y}\phi_{\mathrm{S}}(x)\,, \tag{2}$$

$$\langle 0|\bar{d}(y)\gamma_5\sigma_{\mu\nu} u(0)|\pi^+(P)\rangle = -\frac{\mathrm{i}}{6} f_\pi m_0 \times \left(1 - \frac{M_\pi^2}{m_0^2}\right)(P_\mu y_\nu - P_\nu y_\mu)\int_0^1 \mathrm{d}x \mathrm{e}^{-\mathrm{i}xP\cdot y}\phi_\sigma(x)\,, \tag{3}$$

where $\phi_{\mathrm{P,S},\sigma}$ and g_π are the distribution amplitudes of unit normalization, f_π the pion decay constant, M_π the pion mass, x the momentum fraction associated with the $\bar{d}$ quark evaluated at the coordinate y. The Wilson links that render the above non-local matrix elements gauge invariant are not shown explicitly. It is easy to observe that the contribution from ϕ_P, independent of the pion mass, is twist-2, and the contribution from g_π is twist-4 because of the factor M_π^2. The contributions from the pseudo-scalar (PS) distribution

amplitude $\phi_{\rm S}$ and from the pseudo-tensor (PT) distribution amplitude ϕ_σ, proportional to the chiral enhancing scale m_0, are twist-3.

We concentrate on the factorization of the two-parton twist-3 distribution amplitudes $\phi_{\rm S}$ and ϕ_σ from the processes $\pi\gamma^*\to\pi$ and $B\to\pi l\nu$. We shall not consider the three-parton twist-3 distribution amplitudes here, since their contributions to exclusive processes are suppressed by the strong coupling constant and of higher power. The reason is as follows: after factorizing the corresponding infrared divergences to all orders, the contribution is written as a convolution of a hard amplitude with the three-parton twist-3 distribution amplitudes. The hard amplitude contains one more attachment from the extra parton (gluon) compared to that in the two-parton case. The attachment introduces one more power of the coupling constant, and one more hard propagator proportional to $1/Q$, where Q is a large scale characterizing the hard amplitude. Hence, a three-parton hard amplitude is at least down by a power of the coupling constant and a power of $1/Q$ compared to the leading-order leading-twist hard amplitude. Moreover, the three-parton twist-3 distribution amplitudes should be considered along with the two-parton $k_{\rm T}$ distribution amplitudes, which form a complete gauge-invariant set.

Non-perturbative dynamics is reflected by infrared divergences of radiative corrections in perturbation theory. There are two types of infrared divergences, soft and collinear. Soft divergences come from the region of a loop momentum l, where all its components diminish. Collinear divergences are associated with a massless quark of momentum $P\sim(Q,0,0_{\rm T})$. In the soft region and in the collinear region with l parallel to P, the components of l behave like

$$l^\mu=(l^+,l^-,l_{\rm T})\sim(\lambda,\lambda,\lambda)\,,\quad l^\mu\sim(Q,\lambda^2/Q,\lambda)\,,\quad(4)$$

respectively, where the light-cone coordinates have been adopted, and λ is a small hadronic scale. In both regions the invariant mass of the radiated gluon diminishes as λ^2, and the corresponding loop integrand may diverge as $1/\lambda^4$. As the phase space for loop integration vanishes like $d^4l\sim\lambda^4$, logarithmic divergences are generated.

In this paper we shall derive the collinear factorization formula for the scattering process $\pi\gamma^*\to\pi$, which involves the pion form factor, at twist-3 by means of the Ward identity. The chirally enhanced contributions to the pion form factor have been calculated in [10] without proving their factorization theorem. It will be shown that soft divergences cancel and collinear divergences, factored out of the processes order by order, are absorbed into the two-parton twist-3 pion distribution amplitudes defined by the non-local matrix elements,

$$\begin{aligned}&\phi_{\rm S}(x)\\&=\mathrm{i}\frac{P^+}{m_0}\int\frac{\mathrm{d}y^-}{2\pi}\mathrm{e}^{\mathrm{i}xP^+y^-}\langle0|\bar d(y^-)\gamma_5\\&\quad\times W_{n_-}(y^-)u(0)|\pi^+(P)\rangle,\\&\phi_{\rm T}(x)\\&\equiv\frac{1}{6}\frac{\mathrm{d}}{\mathrm{d}x}\phi_\sigma(x)\\&=\mathrm{i}\frac{P^+}{m_0}\int\frac{\mathrm{d}y^-}{2\pi}\mathrm{e}^{\mathrm{i}xP^+y^-}\langle0|\bar d(y^-)\gamma_5(\not n_+\not n_--1)\\&\quad\times W_{n_-}(y^-)u(0)|\pi^+(P)\rangle\,,\end{aligned}\quad(5)$$

where $n_+=(1,0,0_{\rm T})$ and $n_-=(0,1,0_{\rm T})$ are dimensionless vectors on the light cone, $W_{n_-}(y^-)$ the Wilson line integral,

$$W_{n_-}(y^-)=\mathcal{P}\exp\left[-\mathrm{i}g\int_0^{y^-}\mathrm{d}zn_-\cdot A(zn_-)\right],\quad(6)$$

with the symbol $\mathcal{P}$ standing for the path ordering, and the pion decay constant f_π has been omitted. The definition of the hard amplitudes at each order will be given as a result of the proof.

We then prove the collinear factorization theorem for the semileptonic decay $B\to\pi l\nu$, whose topology is similar to the scattering process $\pi\gamma^*\to\pi$. In the heavy quark limit the mass difference between the B meson and the b quark, $\bar\Lambda=M_B-m_b$, represents a small scale. Assuming the hard scale to be of $O(\sqrt{\bar\Lambda M_B})$, the soft divergences do not cancel on the B meson side, and the B meson distribution amplitudes are introduced to absorb the soft divergences. The distinction between the factorization of soft divergences for the B meson distribution amplitudes and the factorization of collinear divergences for the pion distribution amplitudes will be explained. It will be shown that the two-parton twist-3 pion distribution amplitudes derived from the scattering $\pi\gamma^*\to\pi$ and from the decay $B\to\pi l\bar\nu$ are identical as defined by (5). That is, the universality of hadron distribution amplitudes is confirmed.

There are different opinions on whether the transverse degrees of freedom of partons should be involved in exclusive B meson decays [11–13]. The conclusion drawn in [12,13] that the parton transverse momenta $k_{\rm T}$ are not necessary is based on the analysis of the $B\to\gamma l\nu$ decay, for which the collinear factorization formula does not develop an end-point singularity. When end-point singularities appear [14–16], for example, in the collinear factorization formulas of semileptonic and non-leptonic decays, the region with a small momentum fraction x becomes important. In this end-point region the parton $k_{\rm T}$ should be taken into account, and the $k_{\rm T}$ factorization theorem [17,18] is more appropriate. Here we shall derive the collinear factorization formalism for exclusive B meson decays. The $k_{\rm T}$ dependence can be introduced straightforwardly following the procedure in [19].

We emphasize that the proof of the factorization theorem is not the whole story of PQCD. The double logarithms $\alpha_{\rm s}\ln^2x$ appearing in higher-order corrections to exclusive B meson decays have been observed [11,12,20–22]. When the end-point region is important, $\alpha_{\rm s}\ln^2x$ cannot be treated as a small expansion parameter, and should be summed to all orders. A systematic treatment of these logarithms has been proposed by grouping them into a quark jet function [23], whose dependence on x is governed by an evolution equation [21]. A Sudakov factor, obtained by solving the evolution equation, decreases fast at the end point. Moreover, if the $k_{\rm T}$ factorization theorem is adopted, $k_{\rm T}$ resummation is also required, which leads to another

Sudakov factor describing the parton distribution in $k_{\rm T}$. Therefore, in a self-consistent analysis the original factorization formulas should be convoluted with the above two Sudakov factors. It turns out that the end-point singularities do not exist [24], and an arbitrary infrared cut-off for the momentum fraction x [14,25] is not required.

In the framework of soft-collinear effective theory (SCET) [26,27], an effective Lagrangian with high-energy modes integrated out has been constructed. This SCET Lagrangian provides a simple guideline for deriving a factorization formula by counting the powers of effective operators: start with an effective operator relevant for a high-energy QCD process, and draw the diagrams based on the SCET Lagrangians. Those effective diagrams, whose contributions scale like the power the same as of the operator, contribute to the matrix element formed by the operator. This matrix element is identified as the non-perturbative distribution amplitude, which collects the infrared divergences in the process. The Wilson coefficient (the hard amplitude) associated with the considered operator is then obtained by subtracting the effective diagrams from the full diagrams (the matching between the full theory and the effective theory). An example for the application of SCET, the collinear factorization of the $B \to D\pi$ decays, can be found in [28]. We shall compare the above formalism with ours at the end of this paper. For a detailed comparison, refer to [29].

We mention the opinion from the QCD-improved factorization (QCDF) [25], which claims that the $B \to \pi$ form factor, suffering the end-point singularity in collinear factorization, is dominated by soft dynamics. For a debate on this issue, refer to [13,30]. We have explained that the opposite conclusions on the dominant dynamics in exclusive B meson decays are attributed to the different theoretical frameworks [31]: a transition form factor is factorizable in PQCD, i.e., in $k_{\rm T}$ factorization as explained above, not factorizable in QCDF, i.e., in collinear factorization (speaking of only the leading contribution) [25], and partially factorizable in SCET [32] (non-singular and singular pieces in collinear factorization are written into factorizable and non-factorizable forms, respectively). There is no conflict at all among these observations. It has been pointed out that the collinear factorization and the $k_{\rm T}$ factorization lead to different phenomenological predictions for non-leptonic B meson decays, such as the CP asymmetries in the $B \to \pi^+\pi^-$ modes [19,33,34]. Therefore, it is expected that the comparison with experimental data can discriminate the above approaches.

In Sect. 2 we derive the $O(\alpha_{\rm s})$ factorization of the collinear divergences in the process $\pi\gamma^* \to \pi$. The delicate summation of a complete set of diagrams for achieving the factorizations in momentum, spin, and color spaces is emphasized. The all-order proof based on the Ward identity is presented in Sect. 3. The absence of the soft divergences is also shown. The technique is then generalized to the decay $B \to \pi l\nu$ in Sect. 4. The factorizations of soft divergences for the B meson distribution amplitudes and of collinear divergences for the pion distribution amplitudes are compared. Section 5 is the conclusion. We refer the detailed calculations of the $O(\alpha_{\rm s})$ infrared divergences in the above two processes to Appendices A, B, and C.

2 $O(\alpha_{\rm s})$ factorization of $\pi\gamma^* \to \pi$

We start with the two-parton twist-3 factorization of the process $\pi\gamma^* \to \pi$ at the one-loop level, which will serve as a starting point of the all-order proof. The momentum P_1 (P_2) of the initial-state (final-state) pion is parameterized as

$$P_1 = (P_1^+, 0, \mathbf{0}_{\rm T}) = \frac{Q}{\sqrt{2}}(1, 0, \mathbf{0}_{\rm T})\,,$$
$$P_2 = (0, P_2^-, \mathbf{0}_{\rm T}) = \frac{Q}{\sqrt{2}}(0, 1, \mathbf{0}_{\rm T})\,. \tag{7}$$

Consider the kinematic region with large $Q^2 = -q^2$, $q = P_2 - P_1$ being the momentum transfer from the virtual photon, where PQCD is applicable. The lowest-order diagrams with the valence quarks being the external particles are displayed in Fig. 1. The lower valence quark (an anti-quark $\bar{d}$) in the initial-state pion carries the fractional momentum x_1P_1. The lower valence quark in the final state carries the fractional momentum x_2P_2. Figure 1a gives the amplitude,

$$G^{(0)}(x_1, x_2) = \frac{\rm i}{2} e g^2 C_F \times \frac{\bar{d}_i(x_1P_1) I_{ij} [\gamma^\nu d(x_2P_2) \bar{u}(\bar{x}_2P_2) \gamma_\nu (\not{P}_2 - x_1 \not{P}_1) \gamma_\mu]_{jl}}{(P_2 - x_1P_1)^2 (x_1P_1 - x_2P_2)^2} \times I_{lk} u_k(\bar{x}_1P_1)\,, \tag{8}$$

with $\bar{x}_{1(2)} \equiv 1 - x_{1(2)}$, the identity matrix I, and the color factor C_F, where the averages over spins and colors of the u and $\bar{d}$ quarks have been done. The u and $\bar{d}$ quark fields obey the equations of motion,

$$\bar{x}_1 \not{P}_1 u(\bar{x}_1P_1) = 0\,, \quad \bar{d}(x_1P_1) x_1 \not{P}_1 = 0\,, \tag{9}$$

where the quark masses m_u and m_d have been neglected in high-energy scattering.

Insert the Fierz identity,

$$\begin{aligned} I_{ij} I_{lk} &= \frac{1}{4} I_{ik} I_{lj} + \frac{1}{4} (\gamma_\alpha)_{ik} (\gamma^\alpha)_{lj} + \frac{1}{4} (\gamma_5 \not{n}_-)_{ik} (\not{n}_+ \gamma_5)_{lj} \\ &\quad + \frac{1}{4} (\gamma_5)_{ik} (\gamma_5)_{lj} \\ &\quad + \frac{1}{4} [\gamma_5 (\not{n}_+ \not{n}_- - 1)]_{ik} [(\not{n}_+ \not{n}_- - 1) \gamma_5]_{lj}\,, \end{aligned} \tag{10}$$

into (8) to separate the fermion flow. Different terms in the above identity correspond to contributions of different twists. The PS structure proportional to γ_5 and the PT structure proportional to $\gamma_5(\not{n}_+ \not{n}_- - 1)$ lead to the twist-3 contributions. Equation (10) is a modified version appropriate for extracting collinear divergences [24]: the choice of the PT structure in (10) and the ordinary one

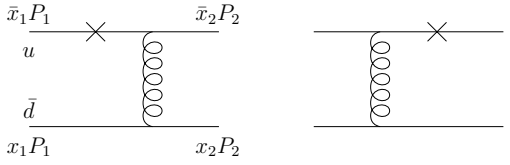

Fig. 1a,b. Lowest-order diagrams for $\pi\gamma^* \to \pi$ ($B \to \pi l\nu$), where the symbol $\times$ represents the virtual photon (weak decay) vertex

$(\gamma_5\sigma^{\alpha\beta})_{ik}(\sigma_{\alpha\beta}\gamma_5)_{lj}$ are equivalent. The PS and PT contributions to the process $\pi\gamma^* \to \pi$ must be included simultaneously in order to form the gauge interaction vertex of a pseudo-scalar particle, which is proportional to $(P_1+P_2)_\mu$.

The insertion on the initial-state side gives

$$G^{(0)}(x_1,x_2) = \int \mathrm{d}\xi_1 \left[\phi_{\mathrm{S}}^{(0)}(x_1,\xi_1)H_{\mathrm{S}}^{(0)}(\xi_1,x_2) + \phi_{\mathrm{T}}^{(0)}(x_1,\xi_1)H_{\mathrm{T}}^{(0)}(\xi_1,x_2)\right] . \tag{11}$$

The functions $\phi_{\mathrm{S(T)}}^{(0)}$ and $H_{\mathrm{S(T)}}^{(0)}$,

$$\begin{aligned}
&\phi_{\mathrm{S}}^{(0)}(x_1,\xi_1) = \frac{1}{4m_0}\bar{d}(x_1P_1)\gamma_5 u(\bar{x}_1P_1)\delta(\xi_1-x_1)\,,\\
&\phi_{\mathrm{T}}^{(0)}(x_1,\xi_1)\\
&= \frac{1}{4m_0}\bar{d}(x_1P_1)\gamma_5(\not{n}_+\not{n}_- - 1)u(\bar{x}_1P_1)\delta(\xi_1-x_1)\,,\\
&H_{\mathrm{S}}^{(0)}(\xi_1,x_2) = \frac{\mathrm{i}}{2}eg^2C_Fm_0\\
&\quad\times\frac{\mathrm{tr}[\gamma^\nu d(x_2P_2)\bar{u}(\bar{x}_2P_2)\gamma_\nu(\not{P}_2-\xi_1\not{P}_1)\gamma_\mu\gamma_5]}{(P_2-\xi_1P_1)^2(\xi_1P_1-x_2P_2)^2}\,,\\
&H_{\mathrm{T}}^{(0)}(\xi_1,x_2) = \frac{\mathrm{i}}{2}eg^2C_Fm_0\\
&\quad\times\mathrm{tr}[\gamma^\nu d(x_2P_2)\bar{u}(\bar{x}_2P_2)\gamma_\nu(\not{P}_2-\xi_1\not{P}_1)\\
&\qquad\times\gamma_\mu(\not{n}_+\not{n}_- - 1)\gamma_5]\\
&\quad/((P_2-\xi_1P_1)^2(\xi_1P_1-x_2P_2)^2)\,,
\end{aligned} \tag{12}$$

define the lowest-order perturbative PS (PT) distribution amplitude and the corresponding hard amplitude, respectively. The meaning of the variable ξ_1, regarded as a momentum fraction modified by collinear gluon exchanges, will become clear below.

Consider the $O(\alpha_{\mathrm{s}})$ radiative corrections to Fig. 1a in the covariant (Feynman) gauge, which are shown in Fig. 2, and identify their infrared divergences. Self-energy corrections to the internal lines, giving a next-to-leading-order hard amplitude, are not included. Here we summarize only the results of the $O(\alpha_{\mathrm{s}})$ factorization, and leave the details to Appendix A. It will be shown that all the diagrams in Fig. 2 can be written as the convolution of the lowest-order hard amplitudes $H_{\mathrm{S,T}}^{(0)}$ in (12) with the $O(\alpha_{\mathrm{s}})$ divergent

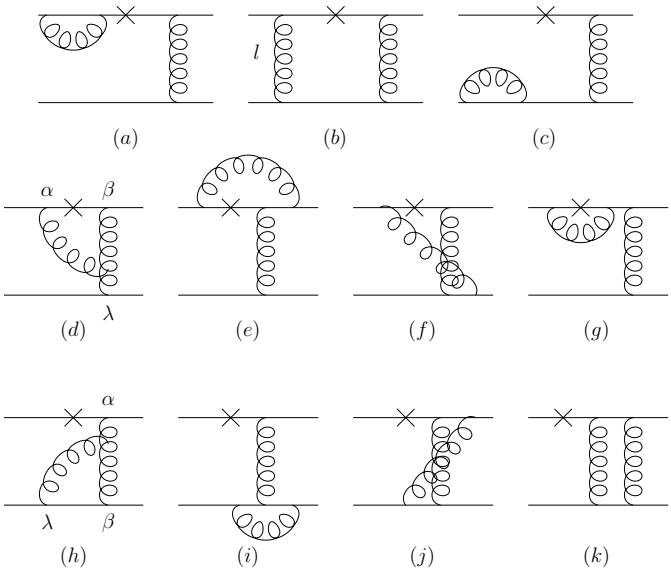

Fig. 2a–k. $O(\alpha_{\mathrm{s}})$ radiative corrections to Fig. 1a

distribution amplitudes $\phi_{\mathrm{S,T}}^{(1)}$ in the collinear region with the loop momentum l parallel to P_1. The expressions of $\phi_{\mathrm{S,T}}^{(1)}$ will provide a basis of constructing the all-order definitions of the two-parton twist-3 distribution amplitudes as non-local matrix elements.

Figures 2a–c are the two-particle reducible diagrams with the additional gluon attaching the two valence quarks of the initial state. It has been known that soft divergences cancel among these diagrams. The reason for this cancellation is that soft gluons, being huge in space-time, do not resolve the color structure of the pion. Collinear divergences in Figs. 2a–c do not cancel, since the loop momentum flows into the internal lines in Fig. 2b, but not in Figs. 2a,c. Inserting the Fierz identity into Figs. 2a–c, we obtain the approximate loop integrals in the collinear region,

$$I^{(a),(b),(c)} \approx \sum_{n=\mathrm{S,T}}\int \mathrm{d}\xi_1\phi_{na,nb,nc}^{(1)}(x_1,\xi_1)H_n^{(0)}(\xi_1,x_2)\,, \tag{13}$$

respectively. The $O(\alpha_{\mathrm{s}})$ PS pieces,

$$\begin{aligned}
&\phi_{\mathrm{S}a}^{(1)}(x_1,\xi_1) = \frac{-g^2C_F}{8m_0}\\
&\quad\times\int\frac{\mathrm{d}^4l}{(2\pi)^4}\bar{d}(x_1P_1)\gamma_5\frac{\mathrm{i}}{\bar{x}_1\not{P}_1}\gamma_\beta\frac{\bar{x}_1\not{P}_1+\not{l}}{(\bar{x}_1P_1+l)^2}\\
&\qquad\times\gamma^\beta u(\bar{x}_1P_1)\frac{1}{l^2}\delta(\xi_1-x_1)\,,
\end{aligned} \tag{14}$$

$$\begin{aligned}
&\phi_{\mathrm{S}b}^{(1)}(x_1,\xi_1)\\
&= \frac{\mathrm{i}g^2C_F}{4m_0}\int\frac{\mathrm{d}^4l}{(2\pi)^4}\bar{d}(x_1P_1)\gamma_\beta\frac{x_1\not{P}_1-\not{l}}{(x_1P_1-l)^2}\\
&\quad\times\gamma_5\frac{\bar{x}_1\not{P}_1+\not{l}}{(\bar{x}_1P_1+l)^2}\gamma^\beta u(\bar{x}_1P_1)\frac{1}{l^2}\delta\left(\xi_1-x_1+\frac{l^+}{P_1^+}\right),
\end{aligned} \tag{15}$$

$\phi_{\mathrm{S}c}^{(1)}(x_1,\xi_1)$

$$= \frac{g^2 C_F}{8m_0}\int \frac{\mathrm{d}^4 l}{(2\pi)^4}\bar{d}(x_1P_1)\gamma_\beta \frac{x_1\not{P}_1 - \not{l}}{(x_1P_1-l)^2}\gamma^\beta \frac{-\mathrm{i}}{x_1\not{P}_1} \times\gamma_5 u(\bar{x}_1P_1)\frac{1}{l^2}\delta(\xi_1-x_1)\,, \quad (16)$$

and the PT pieces with γ_5 in the above expressions being replaced by $\gamma_5(\not{n}_+\not{n}_- - 1)$, contain the collinear (logarithmic) divergences in Figs. 2a,b,c, respectively. Note that the momentum fraction x_1 in Fig. 2b has been modified into $\xi_1 = x_1 - l^+/P_1^+$, because the loop momentum l flows through the hard gluon.

We then consider the factorization of the loop integrals associated with the two-particle irreducible diagrams in Figs. 2d–g. Here we summarize only the results of the factorization, and refer the detail to Appendix A. Summing the contributions from Figs. 2d–g, we arrive at

$$\sum_{i=(\mathrm{d})}^{(g)} I^i \approx \sum_{n=\mathrm{S,T}}\int \mathrm{d}\xi_1 \phi_{nu}^{(1)}(x_1,\xi_1)H_n^{(0)}(\xi_1,x_2)\,, \quad (17)$$

with the PS piece being associated with the collinear gluon emitted from the incoming u quark,

$$\phi_{\mathrm{S}u}^{(1)}(x_1,\xi_1) = \frac{-\mathrm{i}g^2C_F}{4m_0} \times\int \frac{\mathrm{d}^4 l}{(2\pi)^4}\bar{d}(x_1P_1)\gamma_5\frac{\bar{x}_1\not{P}_1 + \not{l}}{(\bar{x}_1P_1+l)^2}\gamma^\beta u(\bar{x}_1P_1)\frac{1}{l^2}\frac{n_{-\beta}}{n_-\cdot l} \times\left[\delta(\xi_1-x_1) - \delta\left(\xi_1 - x_1 + \frac{l^+}{P_1^+}\right)\right]. \quad (18)$$

The corresponding PT pieces are defined similarly with γ_5 in the above expressions being replaced by $\gamma_5(\not{n}_+\not{n}_- - 1)$.

Some remarks are in order.

(i) Figures 2d,g are free of soft divergences, because the additional gluon attaches the virtual gluon and the virtual quark, respectively. The soft divergences cancel between Figs. 2e,f.

(ii) Figures 2d–g possess different color factors due to different color flows. The net color factor C_F is a consequence of summing a set of diagrams, and implies the factorization of the distribution amplitude from other parts of the process in color space.

(iii) The Feynman rule $n_{-\beta}/n_-\cdot l$, coming from the eikonal approximation for the $l \parallel P_1$ configuration, could be generated by a Wilson line in the direction of n_-. This factor will not appear, if the proof is performed in the axial gauge $n_-\cdot A = 0$.

(iv) The first and second δ-functions correspond to the cases without and with the loop momentum l flowing through the internal lines, respectively; that is, to Figs. 3a,b, respectively, where the double lines represent the Wilson lines mentioned above.

The analysis of Figs. 2h–k is similar. The soft divergences cancel among these diagrams. Summing Figs. 2h–k, we derive the correct color factor:

$$\sum_{i=(h)}^{(k)} I^i \approx \sum_{n=\mathrm{S,T}}\int \mathrm{d}\xi_1 \phi_{n\bar{d}}^{(1)}(x_1,\xi_1)H_n^{(0)}(\xi_1,x_2)\,, \quad (19)$$

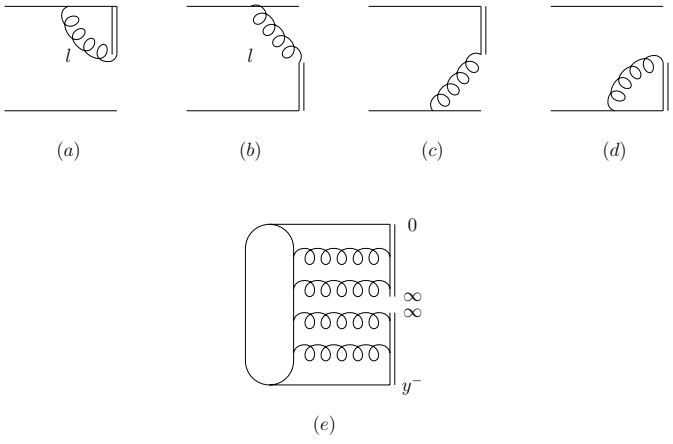

Fig. 3. a–d Infrared divergent diagrams factored out of Fig. 2d–k. **e** The graphic definition of the two-parton twist-3 pion distribution amplitudes

where the PS piece,

$$\phi_{\mathrm{S}\bar{d}}^{(1)}(x_1,\xi_1) = \frac{\mathrm{i}g^2C_F}{4m_0} \times\int \frac{\mathrm{d}^4 l}{(2\pi)^4}\bar{d}(x_1P_1)\gamma^\beta \frac{x_1\not{P}_1 - \not{l}}{(x_1P_1-l)^2}\gamma_5 u(\bar{x}_1P_1)\frac{1}{l^2}\frac{n_{-\beta}}{n_-\cdot l} \times\left[\delta(\xi_1-x_1) - \delta\left(\xi_1 - x_1 + \frac{l^+}{P_1^+}\right)\right], \quad (20)$$

is associated with the collinear gluon emitted from the $\bar{d}$ quark. The first and second δ-functions in (20) correspond to Figs. 3d,c respectively.

The sum of (13), (17) and (19) leads to

$$\sum_{i=(a)}^{(k)} I^i \approx \sum_{n=\mathrm{S,T}}\int \mathrm{d}\xi_1 \phi_n^{(1)}(x_1,\xi_1)H_n^{(0)}(\xi_1,x_2)\,, \quad (21)$$

where $\phi_{\mathrm{S}}^{(1)}$ and $\phi_{\mathrm{T}}^{(1)}$ are represented by the $O(\alpha_{\mathrm{s}})$ terms of the non-local matrix elements with the structures γ_5 and $\gamma_5(\not{n}_+\not{n}_- - 1)$ sandwiched,

$$\phi_{\mathrm{S}}(x,\xi) = \mathrm{i}\frac{P^+}{m_0}\int\frac{\mathrm{d}y^-}{2\pi}\mathrm{e}^{\mathrm{i}\xi P^+y^-}\langle 0|\bar{d}(y^-)\gamma_5 \times W_{n_-}(y^-)u(0)|u(\bar{x}P)\bar{d}(xP)\rangle\,,$$

$$\phi_{\mathrm{T}}(x,\xi) = \mathrm{i}\frac{P^+}{m_0}\int\frac{\mathrm{d}y^-}{2\pi}\mathrm{e}^{\mathrm{i}\xi P^+y^-}\langle 0|\bar{d}(y^-)\gamma_5(\not{n}_+\not{n}_- - 1) \times W_{n_-}(y^-)u(0)|u(\bar{x}P)\bar{d}(xP)\rangle\,, \quad (22)$$

respectively. Expanding the quark field $\bar{d}(y^-)$ and the path-ordered exponential (Wilson line) into powers of y^-, the above matrix elements can be expressed as a series of the covariant derivatives $(D^+)^n\bar{d}(0)$, and are gauge invariant. The integral over z contains two pieces: for the upper Wilson

line in Fig. 3a, z runs from 0 to ∞. For the lower Wilson line in Fig. 3b, z runs from ∞ back to y^-. The light-cone coordinate $y^- \neq 0$ reflects the fact that the collinear divergences in Fig. 2 do not cancel. Notice the different kets $|\pi^+(P)\rangle$ and $|u(\bar{x}P)\bar{d}(xP)\rangle$ in (5) and (22), respectively. Equation (22) plays the role of an infrared regulator for parton-level diagrams. A hard amplitude, obtained by subtracting (22) from the parton-level diagrams, then corresponds to the regularized parton-level diagrams. After determining the gauge-invariant infrared-finite hard amplitude $H(x)$, we convolute it with the physical two-parton twist-3 pion distribution amplitudes defined in (5) and graphically shown in Fig. 3e. Models for the two-parton twist-3 pion distribution amplitudes have been derived using QCD sum rules [9].

It is easy to confirm that $\phi^{(1)}_{\rm S,T}$ is reproduced by the perturbative expansion of the matrix elements in (22). Take (18) as an example. Fourier transforming the gauge field $A(zn_-)$ into $\tilde{A}(l)$, we have

$$-\mathrm{i}g\int_0^\infty \mathrm{d}z\,\exp[\mathrm{i}z(n_-\cdot l+\mathrm{i}\epsilon)]n_-\cdot\tilde{A}(l) = g\frac{n_-^\alpha}{n_-\cdot l}\tilde{A}_\alpha(l)\,. \tag{23}$$

The field $\tilde{A}_\alpha(l)$, contracted with another gauge field associated with the u quark, gives the gluon propagator in Fig. 3a. It is then realized that the eikonal propagator is generated by the path-ordered exponential. The second piece of the Wilson line corresponds to the second term in (18):

$$-\mathrm{i}g\int_\infty^{y^-} \mathrm{d}z\,\exp[\mathrm{i}z(n_-\cdot l+\mathrm{i}\epsilon)]n_-\cdot\tilde{A}(l) = -g\frac{n_-^\alpha}{n_-\cdot l}\exp(\mathrm{i}l^+y^-)\tilde{A}_\alpha(l)\,, \tag{24}$$

where the extra Fourier factor $\exp(\mathrm{i}l^+y^-)$ leads to the function $\delta(\xi - x + l^+/P_1^+)$. The field $\tilde{A}_\alpha(l)$, contracted with another gauge field associated with the u quark, gives the gluon propagator in Fig. 3b. The Feynman rules for (20) can be reproduced in a similar way, where $\tilde{A}_\alpha(l)$ is contracted with another gauge field associated with the $\bar{d}$ quark. Equations (14)–(16) are derived by contracting the gluon fields associated with the u and $\bar{d}$ quarks.

The above derivation also applies straightforwardly to the factorization of the collinear divergences associated with the final state, which arise from the region with the loop momentum parallel to P_2. Hence, we have an expression similar to (21), $\sum_{m=\rm S,T} H_m^{(0)}\otimes\phi_m^{(1)}$, where $\phi_m^{(1)}$ is the final-state distribution amplitude, and $H_m^{(0)}$ is the hard amplitude with the Fierz identity inserted into the final-state side of $H^{(0)}$. The symbol $\otimes$ represents the convolution in the variable ξ_2. The momentum fraction associated with the final state will be modified into $\xi_2 = x_2 - l^-/P_2^-$ by the collinear gluons parallel to P_2, if the loop momentum l flows through the hard amplitude $H_m^{(0)}$.

The $O(\alpha_{\rm s})$ radiative corrections to Fig. 1b are displayed in Fig. 4. The factorization of the collinear divergences from these diagrams is referred to Appendix B. The result is similar to (21) but without the PT contributions, because of $\gamma^\nu(\not{n}_+\ \not{n}_- - 1)\gamma_\nu = 0$, where the gamma matrices γ^ν and γ_ν come from the gluon vertices in Fig. 1b. Hence, we derive, from Fig. 4,

$$\sum_{i=(a)}^{(k)} I^i \approx \int \mathrm{d}\xi_1\phi_{\rm S}^{(1)}(x_1,\xi_1)H_{\rm S}^{(0)}(\xi_1,x_2)\,, \tag{25}$$

where the definition of the $O(\alpha_{\rm s})$ PS distribution amplitude $\phi_{\rm S}^{(1)}$ is the same as in (22). This is expected due to the universality.

In summary, the $O(\alpha_{\rm s})$ factorization of the process $\pi\gamma^*\to\pi$ is written as

$$G^{(1)} = \sum_{n=\rm S,T}\phi_n^{(1)}\otimes H_n^{(0)} + \sum_{m=\rm S,T} H_m^{(0)}\otimes\phi_m^{(1)} + H^{(1)}, \tag{26}$$

where $G^{(1)}$ denotes the complete set of the $O(\alpha_{\rm s})$ corrections, and $H_{n,m}^{(0)}$ receive the contributions from both Figs. 1a,b now. The first term on the right-hand side of the above expression does not contain the collinear divergences from the loop momentum l parallel to P_2. In this region l^+ is negligible, ξ_1 approaches x_1, and the corresponding collinear divergences cancel in $\phi_n^{(1)}$. For the similar reason, the second term on the right-hand side of (26) does not contain the collinear divergences from l parallel to P_1. That is, the initial-state and final-state collinear divergences in $G^{(1)}$ have been completely factorized into the first and second terms on the right-hand side of (26), respectively. The $O(\alpha_{\rm s})$ hard amplitude $H^{(1)}$, defined via (26), is infrared finite. Note that $H^{(1)}$ contains the self-energy corrections to the internal lines.

Summing (26) and the lowest-order diagrams $G^{(0)}$, the factorization formula for the two-parton twist-3 contributions to the process $\pi\gamma^*\to\pi$ is given, up to $O(\alpha_{\rm s})$, by

$$G^{(0)} + G^{(1)}$$

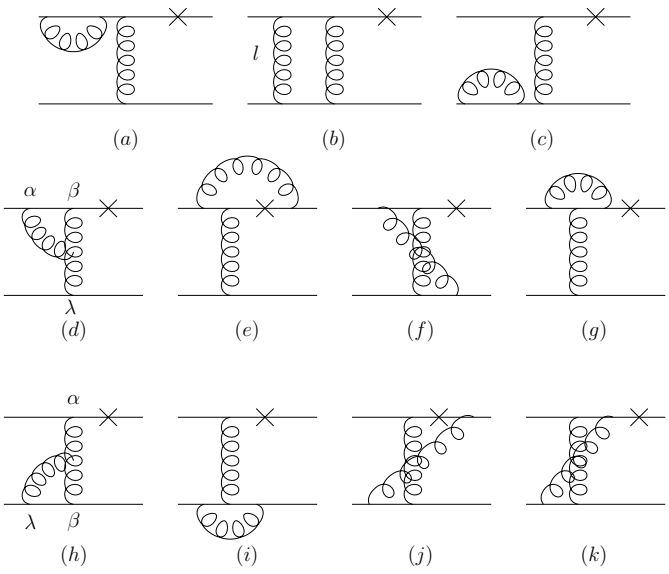

Fig. 4a–k. $O(\alpha_{\rm s})$ radiative corrections to Fig. 1b

$$= \sum_{n,m=\mathrm{S,T}} (\phi_n^{(0)} + \phi_n^{(1)}) \otimes (H_{nm}^{(0)} + H_{nm}^{(1)}) \otimes (\phi_m^{(0)} + \phi_m^{(1)}) , \quad (27)$$

where the trivial factorizations,

$$H_n^{(0)} = \sum_{m=\mathrm{S,T}} H_{nm}^{(0)} \otimes \phi_m^{(0)} ,$$
$$H_m^{(0)} = \sum_{n=\mathrm{S,T}} \phi_n^{(0)} \otimes H_{nm}^{(0)} ,$$
$$H^{(1)} = \sum_{n,m=\mathrm{S,T}} \phi_n^{(0)} \otimes H_{nm}^{(1)} \otimes \phi_m^{(0)} , \quad (28)$$

have been adopted. The last formula in (28) defines the $O(\alpha_s)$ hard amplitude $H_{nm}^{(1)}$. The explicit expression of, for example, $H_{SS}^{(0)}$, is given by

$$H_{SS}^{(0)}(\xi_1, \xi_2) = \frac{\mathrm{i}}{2} e g^2 C_F m_0^2 \times \left\{ \frac{\mathrm{tr}[\gamma^\nu \gamma_5 \gamma_\nu (\not{P}_2 - \xi_1 \not{P}_1) \gamma_\mu \gamma_5]}{(P_2 - \xi_1 P_1)^2 (\xi_1 P_1 - \xi_2 P_2)^2} + \frac{\mathrm{tr}[\gamma^\nu \gamma_5 \gamma_\mu (\not{P}_1 - \xi_2 \not{P}_2) \gamma_\nu \gamma_5]}{(P_1 - \xi_2 P_2)^2 (\xi_1 P_1 - \xi_2 P_2)^2} \right\} . \quad (29)$$

It is obvious that the PS and PT structures must be included simultaneously for a complete two-parton twist-3 collinear factorization.

3 All-order factorization of $\pi\gamma^* \to \pi$

In this section we present the all-order proof of the two-parton twist-3 factorization theorem for the process $\pi\gamma^* \to \pi$, and construct the gauge-invariant distribution amplitudes in (22). It has been mentioned in the Introduction that factorizations of a QCD process in momentum, spin, and color spaces require summation of many diagrams, especially at higher orders. The diagram summation can be handled in an elegant way by employing the Ward identity,

$$l^\mu G_\mu(l, k_1, k_2, \ldots, k_n) = 0 , \quad (30)$$

where G_μ represents a physical amplitude with an external gluon carrying the momentum l and with n external quarks carrying the momenta k_1, k_2, …, k_n. All these external particles are on mass shell. The Ward identity can be easily derived by means of the Becchi–Rouet–Stora transformation [35]. We shall employ the similar Ward identity,

$$l_1^\mu G_{\mu\nu}(l_1, l_2, k_1, k_2, \ldots, k_n) l_2^\nu = 0 , \quad (31)$$

where $G_{\mu\nu}$ represents a physical amplitude with two external gluons carrying the momenta l_1 and l_2, and with n external quarks.

We shall prove the two-parton twist-3 factorization theorem for the process $\pi\gamma^* \to \pi$ to all orders by induction. The factorization of the $O(\alpha_s)$ collinear divergences has been worked out in Sect. 2. Assume that the factorization theorem holds up to $O(\alpha_s^N)$:

$$G^{(k)} = \sum_{n',m'=\mathrm{S,T}} \sum_{i=0}^{k} \sum_{j=0}^{k-i} \phi_{n'}^{(i)} \otimes H_{n'm'}^{(k-i-j)} \otimes \phi_{m'}^{(j)} , \quad k = 0, 1, \ldots, N . \quad (32)$$

$G^{(k)}$ denotes the parton-level diagrams of $O(\alpha_s^k)$ with $G^{(0)}$ shown in Fig. 1. The initial-state distribution amplitude $\phi_{n'}^{(i)}$ is defined by the $O(\alpha_s^i)$ terms in the perturbative expansion of (22), and the final-state distribution amplitude $\phi_{m'}^{(j)}$ defined similarly by the complex conjugate of (22). $H_{n'm'}^{(k-i-j)}$ is the remaining $O(\alpha_s^{k-i-j})$ piece of the process, which does not contain infrared divergences. Equation (32) implies that all the initial-state and final-state collinear divergences in $G^{(k)}$ have been collected into $\phi_{n'}^{(i)}$ and $\phi_{m'}^{(j)}$ systematically. Inserting the Fierz identity, we also obtain the trivial factorizations of the distribution amplitudes ϕ and the diagrams G at arbitrary orders of α_s, similar to (28):

$$G^{(k)} = \sum_{n,m} \phi_n^{(0)} \otimes G_{nm}^{(k)} \otimes \phi_m^{(0)} , \quad \phi_{n'}^{(i)} = \sum_n \phi_n^{(0)} \otimes \phi_{nn'}^{(i)} ,$$
$$\phi_{m'}^{(j)} = \sum_m \phi_{m'm}^{(j)} \otimes \phi_m^{(0)} . \quad (33)$$

We then have the factorization,

$$G_{nm}^{(k)} = \sum_{n',m'=\mathrm{S,T}} \sum_{i=0}^{k} \sum_{j=0}^{k-i} \phi_{nn'}^{(i)} \otimes H_{n'm'}^{(k-i-j)} \otimes \phi_{m'm}^{(j)} , \quad (34)$$

in which, for example, $\phi_{SS}^{(1)}$ contains the piece $\phi_{SSu}^{(1)}$ extracted from (18),

$$\phi_{SSu}^{(1)}(x_1, \xi_1) = \frac{-\mathrm{i} g^2 C_F}{4 m_0} \int \frac{\mathrm{d}^4 l}{(2\pi)^4} \mathrm{tr} \left[\gamma_5 \frac{\bar{x}_1 \not{P}_1 + \not{l}}{(\bar{x}_1 P_1 + l)^2} \gamma^\beta \gamma_5 \right] \frac{1}{l^2} \frac{n_{-\beta}}{n_- \cdot l} \times \left[\delta(\xi_1 - x_1) - \delta\left(\xi_1 - x_1 + \frac{l^+}{P_1^+} \right) \right] . \quad (35)$$

Below we prove the collinear factorization of the $O(\alpha_s^{N+1})$ diagrams $G^{(N+1)}$, assuming (32) or (34). Look for the radiative gluon in a subset of $O(\alpha_s^{N+1})$ diagrams $G^{(N+1)}$, one of whose ends attaches the outer most vertex on the upper u quark line. Let α denote the outer most vertex, and β denote the attachments of the other end of the identified gluon inside the rest of the diagrams. There are two types of collinear configurations associated with this gluon, depending on whether the vertex β is located on an internal line with the momentum along P_1. The fermion propagator adjacent to the vertex α is proportional to $\not{P}_1$ in the collinear region with the loop momentum l parallel to P_1. If β is not located on a collinear line along P_1, the component γ^+ in γ^α and the minus component of the vertex β give the leading contribution (collinear divergence).

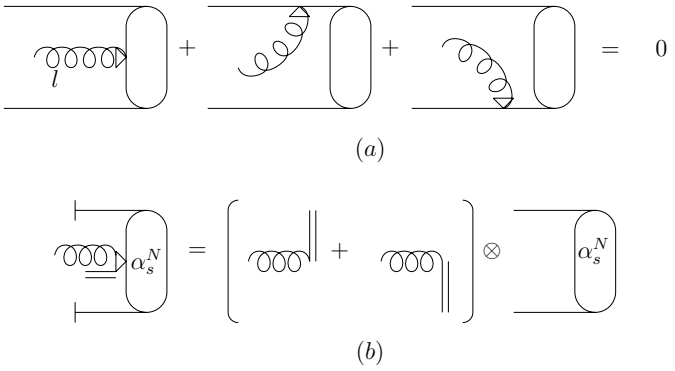

Fig. 5. a The Ward identity. **b** Factorization of $O(\alpha_{\rm s}^{N+1})$ diagrams as a result of **a**

If β is located on a collinear line along P_1, both α and β represent the transverse components for the leading contribution. This configuration is the same as of the self-energy correction to an on-shell particle. According to the above classification, we decompose the tensor $g_{\alpha\beta}$ appearing in the propagator of the identified gluon into [1]

$$g_{\alpha\beta} = \delta_{\alpha+}\delta_{\beta-} - \delta_{\alpha\perp}\delta_{\beta\perp} + \delta_{\alpha-}\delta_{\beta+}\,. \tag{36}$$

The first (second) term on the right-hand side of (36) extracts the aforementioned first (second) type of initial-state collinear divergences. The third term does not contribute due to the equations of motion in (9).

We discuss the factorization of the first type of collinear configurations denoted by $G_{I\cdot}^{(N+1)}$, where the identified collinear gluon is emitted from the initial-state quarks. As stated before, the identified gluon with $\alpha = +$ and $\beta = -$ does not attach the upper or lower quark line directly, which carries the momentum along P_1. That is, those diagrams with Figs. 2a–c as the $O(\alpha_{\rm s})$ subdiagrams are excluded from the set of $G_{I\cdot}^{(N+1)}$ as discussing the first type of collinear configurations. We employ the replacement,

$$\delta_{\alpha+}\delta_{\beta-} \to \frac{n_{-\alpha}l_\beta}{n_-\cdot l}\,, \tag{37}$$

where the light-like vector $n_{-\alpha}$ selects the plus component of γ^α, and l_β selects the minus component of the vertex β in the collinear region. In principle, the arbitrary l_β can attach all the internal lines, no matter they are or are not parallel to P_1. We denote the diagrams with the above replacement as $G_{\|\cdot}^{(N+1)}$. The point is that $G_{I\cdot}^{(N+1)}$ and $G_{\|\cdot}^{(N+1)}$ contain the identical first type of collinear divergences, whose collection will be performed by means of (37).

We then consider Fig. 5a, which contains a complete set of contractions of l_β, since the second and third diagrams have been included, for which l_β selects a plus vertex. The contractions of l_β, represented by arrows, hint the application of the Ward identity in (30) to the case, in which the on-shell external u quark, $\bar{d}$ quark and gluon carry the momenta $\bar{\xi}_1 P_1$, $x_1 P_1$ and l, respectively, with $\bar{\xi}_1 \equiv 1-\xi_1$. The Ward identity states that the expression in Fig. 5a vanishes, and that the first diagram we consider is related to the second and third diagrams, which, after employing (9), give

$$\begin{aligned} & l_\beta \frac{1}{\bar{\xi}_1 \not{P}_1 - \not{l}}\gamma^\beta u(\bar{\xi}_1 P_1) \\ & = \frac{1}{\bar{\xi}_1 \not{P}_1 - \not{l}}(\not{l} - \bar{\xi}_1 \not{P}_1 + \bar{\xi}_1 \not{P}_1)u(\bar{\xi}_1 P_1) = -u(\bar{\xi}_1 P_1)\,, \\ & l_\beta \bar{d}(x_1 P_1)\gamma^\beta \frac{1}{x_1 \not{P}_1 - \not{l}} = -\bar{d}(x_1 P_1)\,, \end{aligned} \tag{38}$$

respectively. The terms $u(\bar{\xi}_1 P_1)$ and $\bar{d}(x_1 P_1)$ at the ends of the above expressions are associated with the $O(\alpha_{\rm s}^N)$ diagrams.

We insert the Fierz identity into Fig. 5a, and factor the lowest-order expressions $\bar{d}(x_1 P_1)\Gamma u(\bar{\xi}_1 P_1)$ with Γ being the PS or PT structure considered in this work. The result is a relation shown in Fig. 5b, where the cuts on the quark lines denote the insertion of the Fierz identity, and the double (Wilson) lines represent $n_{-\alpha}/n_-\cdot l$ in (37). For the case with the identified gluon emitted from the outer most vertex on the u quark line, Fig. 5b implies that the considered $O(\alpha_{\rm s}^{N+1})$ diagrams are factorized into the convolution of the full diagrams $G_n^{(N)}$ with $\phi_{nu}^{(1)}$, n= S, T. The same discussion applies to the factorization of the $O(\alpha_{\rm s}^{N+1})$ diagrams with the collinear gluon emitted from the outer most vertex on the $\bar{d}$ quark line, leading to a convolution of $G_n^{(N)}$ with $\phi_{n\bar{d}}^{(1)}$. Similarly, for the subset $G_{\cdot I}^{(N+1)}$, in which the identified radiative gluon emitted by the outgoing quarks, the collinear divergences are also classified into the two types. In this case it is the third term in (36) that corresponds to the first type of collinear divergences, and the replacement in (37) is modified into

$$\delta_{\alpha-}\delta_{\beta+} \to \frac{n_{+\alpha}l_\beta}{n_+\cdot l}\,. \tag{39}$$

The pieces $\phi_{mu}^{(1)}$ and $\phi_{m\bar{d}}^{(1)}$ containing the identified gluon are factored out of the considered $G_{\cdot\|}^{(N+1)}$ in the collinear region with the loop momentum parallel to P_2.

We conclude that the subset of diagrams $G_{\|\cdot}^{(N+1)}$, in which the replacement in (37) is applied to the initial-state side, and $G_{\cdot\|}^{(N+1)}$, in which the replacement in (39) is applied to the final-state side, are written as

$$G_{\|\cdot}^{(N+1)} \approx \sum_{n={\rm S,T}} \phi_{n\|}^{(1)} \otimes G_n^{(N)}\,, \tag{40}$$

$$G_{\cdot\|}^{(N+1)} \approx \sum_{m={\rm S,T}} G_m^{(N)} \otimes \phi_{m\|}^{(1)}\,, \tag{41}$$

respectively, where $\phi_{n(m)\|}^{(1)}$ represents

$$\phi_{n(m)\|}^{(1)} = \phi_{n(m)u}^{(1)} + \phi_{n(m)\bar{d}}^{(1)}\,. \tag{42}$$

Equation (40) is displayed in Fig. 6. Other diagrams, which do not contain the radiative gluons on either the initial-state side or the final-state side, are self-energy corrections

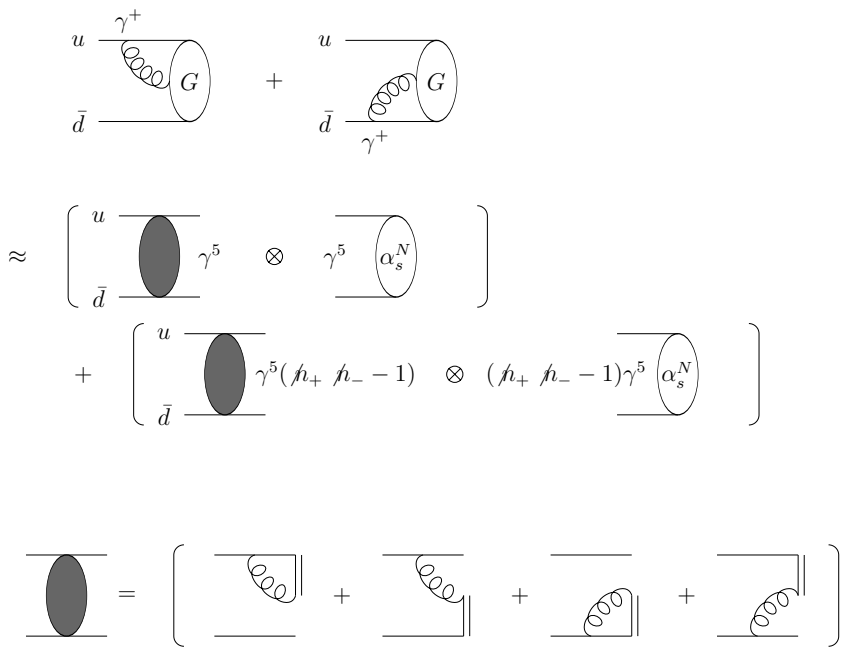

Fig. 6. Factorization of $O(\alpha_s^{N+1})$ diagrams corresponding to (37)

to internal lines. They are infrared finite, and contribute to the $O(\alpha_s^{N+1})$ hard amplitude.

The above procedures are also applicable to the $O(\alpha_s^{j+1})$ initial-state and final-state distribution amplitudes $\phi_n^{(j+1)}$ and $\phi_m^{(j+1)}$. We identify the gluon in a subset of diagrams $\phi_n^{(j+1)}$, one of whose ends attaches the outer most vertex α on the u quark line. The other end attaches the vertex β inside the rest of the diagrams. For the replacements in (37) and (39), which collect the complete first type of collinear divergences, we have a Ward identity similar to Fig. 5a. Figure 5b then leads to the factorizations of the initial-state and final-state distribution amplitudes,

$$\phi_{n\|}^{(j+1)} \approx \sum_{n'=\mathrm{S,T}} \phi_{n'\|}^{(1)} \otimes \phi_{n'n}^{(j)}\,, \tag{43}$$

$$\phi_{m\|}^{(j+1)} \approx \sum_{m'=\mathrm{S,T}} \phi_{mm'}^{(j)} \otimes \phi_{m'\|}^{(1)}\,, \tag{44}$$

where the PS and PT structures in (10) have been inserted.

We sum (40) and (41), and subtract the double-counted diagrams $G_{\| \|}^{(N+1)}$, to which the replacements are applicable to both the initial-state and final-state sides as shown in Fig. 7a. For the factorization of $G_{\| \|}^{(N+1)}$, we rely on the Ward identity in (31). Note that $G_{\| \|}^{(N+1)}$ do not contain the diagrams like Fig. 7b, in which the same gluon is identified in $G_{\|\cdot}^{(N+1)}$ and in $G_{\cdot\|}^{(N+1)}$ simultaneously. This type of diagrams are not double-counted, and (31) does not apply to them. The result is

$$\begin{aligned} & G_{\|\cdot}^{(N+1)} + G_{\cdot\|}^{(N+1)} - G_{\| \|}^{(N+1)} \\ & \approx \sum_{n,m=\mathrm{S,T}} \Big[\phi_{n\|}^{(1)} \otimes G_{nm}^{(N)} \otimes \phi_m^{(0)} + \phi_n^{(0)} \otimes G_{nm}^{(N)} \otimes \phi_{m\|}^{(1)} \\ & \quad - \phi_{n\|}^{(1)} \otimes G_{nm}^{(N-1)} \otimes \phi_{m\|}^{(1)} \Big]\,, \end{aligned} \tag{45}$$

where the trivial factorizations, similar to (28), have been inserted. Substituting (34), (43), and (44) into (45), simple algebra gives

$$\begin{aligned} & G_{\|\cdot}^{(N+1)} + G_{\cdot\|}^{(N+1)} - G_{\| \|}^{(N+1)} \\ & \approx \sum_{n,m=\mathrm{S,T}} \sum_{i=0}^{N} \sum_{j=0}^{N-i} \Big[\phi_{n\|}^{(i+1)} \otimes H_{nm}^{(N-i-j)} \otimes \phi_m^{(j)} \\ & \quad + \phi_n^{(i)} \otimes H_{nm}^{(N-i-j)} \otimes \phi_{m\|}^{(j+1)} \\ & \quad - \phi_{n\|}^{(i+1)} \otimes H_{nm}^{(N-i-j-1)} \otimes \phi_{m\|}^{(j+1)} \Big]\,. \end{aligned} \tag{46}$$

Finally, we recover the tensors $\delta_{\alpha+}\delta_{\beta-}$ and $\delta_{\alpha-}\delta_{\beta+}$ on both sides of (46).

The factorization of the first type of collinear divergences associated with the identified radiative gluon from $G_I^{(N+1)}$, $N \geq 1$, is then given by

$$G_I^{(N+1)} \equiv G_{I\cdot}^{(N+1)} + G_{\cdot I}^{(N+1)} - G_{I\,I}^{(N+1)}$$

(a) (b)

Fig. 7. a A typical diagram of $G_{\| \|}^{(N+1)}$. **b** This diagram does not belong to $G_{\| \|}^{(N+1)}$

$$\approx \sum_{n,m=\mathrm{S,T}} \sum_{i=0}^{N} \sum_{j=0}^{N-i} \Big[\phi_{nI}^{(i+1)} \otimes H_{nm}^{(N-i-j)} \otimes \phi_m^{(j)} + \phi_n^{(i)} \otimes H_{nm}^{(N-i-j)} \otimes \phi_{mI}^{(j+1)} - \phi_{nI}^{(i+1)} \otimes H_{nm}^{(N-i-j-1)} \otimes \phi_{mI}^{(j+1)} \Big] , \quad (47)$$

where $\phi_{nI}^{(i+1)}$ ($\phi_{mI}^{(j+1)}$) contains only the first (third) term in (36).

It is obvious that (47) is not Lorentz covariant, since $G_I^{(N+1)}$, $\phi_{nI}^{(i)}$ and $\phi_{mI}^{(j)}$ include only the first or third term in (36). The Lorentz covariance can be recovered by adding the other two terms in (36) into the tensors for the identified radiative gluons on both sides of (47). Recovering the Lorentz covariance, the second type of collinear configurations associated with the tensor $-\delta_{\alpha\perp}\delta_{\beta\perp}$ is taken into account. We explain the idea by starting with $G_{I\cdot}^{(N+1)}$ as an example, whose factorization is written as

$$G_{I\cdot}^{(N+1)} \approx \sum_{n,m=\mathrm{S,T}} \sum_{i=0}^{N} \sum_{j=0}^{N-i} \phi_{nI}^{(i+1)} \otimes H_{nm}^{(N-i-j)} \otimes \phi_m^{(j)} . \quad (48)$$

We add $G_{\perp\cdot}^{(N+1)}$ on the left-hand side to restore the Lorentz covariance, which contain the identified gluon corresponding to the second term in (36). As stated before, this gluon attaches only the lines parallel to P_1, and generates merely the collinear divergences associated with the initial-state pion. That is, it does not change the hard amplitudes $H_{nm}^{(N-i-j)}$ and the final-state distribution amplitudes $\phi_m^{(j)}$. To recover the Lorentz covariance of the right-hand side, the only option is that the identified gluon contributes the initial-state distribution amplitudes $\phi_{n\perp}^{(i+1)}$. We then have

$$G_{I\cdot}^{(N+1)} + G_{\perp\cdot}^{(N+1)} \approx \sum_{n,m=\mathrm{S,T}} \sum_{i=0}^{N} \sum_{j=0}^{N-i} \phi_n^{(i+1)} \otimes H_{nm}^{(N-i-j)} \otimes \phi_m^{(j)} . \quad (49)$$

The similar procedure applies to $G_{\cdot I}^{(N+1)}$ and $G_{I\,I}^{(N+1)}$: the adding of the tensor $-\delta_{\alpha\perp}\delta_{\beta\perp}$ to $G_{\cdot I}^{(N+1)}$ and $G_{I\,I}^{(N+1)}$ does not change the hard amplitudes. To recover the Lorentz covariance, the only option is that the identified gluon contributes $\phi_{n\perp}^{(i)}$ or $\phi_{m\perp}^{(j)}$. Finally, the complete collinear factorization of the diagrams $G^{(N+1)}$ is given by

$$G^{(N+1)} = \sum_{n,m=\mathrm{S,T}} \sum_{i=0}^{N} \sum_{j=0}^{N-i} \Big[\phi_n^{(i+1)} \otimes H_{nm}^{(N-i-j)} \otimes \phi_m^{(j)} + \phi_n^{(i)} \otimes H_{nm}^{(N-i-j)} \otimes \phi_m^{(j+1)} - \phi_n^{(i+1)} \otimes H_{nm}^{(N-i-j-1)} \otimes \phi_m^{(j+1)} \Big] + F^{(N+1)} , \quad (50)$$

where the $O(\alpha_{\mathrm{s}}^{N+1})$ function $F^{(N+1)}$ contains the infrared-finite diagrams (self-energy corrections to internal lines) mentioned before. Equation (50) can be simplified into

$$G^{(N+1)} = \sum_{n,m=\mathrm{S,T}} \sum_{i=0}^{N+1} \sum_{j=0}^{N+1-i} \phi_n^{(i)} \otimes H_{nm}^{(N+1-i-j)} \otimes \phi_m^{(j)} , \quad (51)$$

with the $O(\alpha_{\mathrm{s}}^{N+1})$ hard amplitude $H_{nm}^{(N+1)}$ being defined via

$$F^{(N+1)} = \sum_{n,m=\mathrm{S,T}} \phi_n^{(0)} \otimes H_{nm}^{(N+1)} \otimes \phi_m^{(0)} . \quad (52)$$

Equation (51) states that all the two-parton twist-3 collinear divergences in the process $\pi\gamma^* \to \pi$ have been factorized into the distribution amplitudes in (22) order by order.

Before closing this section, we prove that soft divergences do not exist in the process $\pi\gamma^* \to \pi$ at the two-parton twist-3 level. The $O(\alpha_{\mathrm{s}})$ soft cancellation has been demonstrated in Sect. 2. Assume that the $O(\alpha_{\mathrm{s}}^N)$ diagrams $G^{(N)}$ do not contain any soft divergences, though they contain collinear ones. They are then dominated by hard dynamics, by collinear dynamics associated with the initial-state pion, and by collinear dynamics associated with the final-state pion. Consider the $O(\alpha_{\mathrm{s}}^{N+1})$ diagrams $G^{(N+1)}$. We look for the gluon radiated from the outer most vertex on the u quark line in the initial state, and adopt the decomposition of the tensor $g_{\alpha\beta}$ in (36). The attachment of a soft gluon to an off-shell internal line does not introduce an infrared divergence, since an off-shell propagator behaves at least like $1/Q$. As the soft gluon attaches a collinear line along P_2, the vertex β must be dominated by the minus component. The gamma matrix γ^α is dominated by the component γ^+ stated above. Therefore, the replacement in (37) still holds for the first term on the right-hand side of (36). Similarly, the second term on the right-hand side of (36) corresponds to the attachment of the soft gluon to a collinear line along P_1. Again, the third term on the right-hand side of (36) does not contribute due to the equations of motion.

The above reasoning indicates that the configurations associated with the identified soft gluon are the same as those associated with the identified collinear gluon. The procedure for deriving the collinear factorization then applies. For the first term in (36), we arrive at (40) for the soft factorization. Because the soft divergences cancel among the diagrams for $\phi_{n\parallel}^{(1)}$ shown in Fig. 3 [between Figs. 3a,b and between Figs. 3c,d], and $G^{(N)}$ do not contain soft divergences by assumption, $G_{\parallel\cdot}^{(N+1)}$, i.e., $G_{I\cdot}^{(N+1)}$ do not either. We then turn to the $O(\alpha_{\mathrm{s}}^{N+1})$ diagrams $G_{\perp\cdot}^{(N+1)}$ associated with the tensor $-\delta_{\alpha\perp}\delta_{\beta\perp}$. If they contain soft divergences, the evaluation of these divergences is not Lorentz covariant, leading to a contradiction. Therefore, the subset of $O(\alpha_{\mathrm{s}}^{N+1})$ diagrams $G^{(N+1)}$ with the identified gluon radiated from the initial-state quarks must be free of soft divergences. The similar argument holds for another subset with the identified gluon radiated from the final-state quarks. These two subsets have covered all the $O(\alpha_{\mathrm{s}}^{N+1})$ diagrams $G^{(N+1)}$, which have potential soft divergences. Hence, we conclude that $G^{(N+1)}$ are free of soft divergences. Extending N to infinity, the absence of the soft

divergences in the diagrams G is proved. We then complete the all-order proof of the two-parton twist-3 collinear factorization theorem for the process $\pi\gamma^* \to \pi$.

4 Factorization of $B \to \pi\ell\nu$

As emphasized in the Introduction, the contributions to the exclusive semileptonic decay $B \to \pi l\nu$ from the two-parton twist-3 pion distribution amplitudes $\phi_{\rm S,T}$ are of the same power as those from the twist-2 one. These contributions are originally proportional to the ratio m_0/M_B. However, the corresponding convolution integral for the $B \to \pi$ form factor is linearly divergent in the collinear factorization theorem, such that it is proportional to the ratio $M_B/\bar{\Lambda}$, if regulated by an effective cut-off $x_c \sim \bar{\Lambda}/M_B$. Combining the two ratios m_0/M_B and $M_B/\bar{\Lambda}$, the two-parton twist-3 contributions are in fact not down by a power of $1/M_B$:

$$\frac{m_0}{M_B}\int_{x_c}^1 {\rm d}x_2 H_{\rm S}(x_2)\phi_{\rm S}(x_2) \sim \frac{m_0}{M_B}\int_{x_c}^1 {\rm d}x_2 \frac{1}{x_2^2} \sim O\left(\frac{m_0}{\bar{\Lambda}}\right), \quad (53)$$

for the asymptotic functional form $\phi_{\rm S} \sim 1$ [9] and $H_{\rm S} \sim 1/x_2^2$ in (70) below. The presence of the linear divergences modifies the naive power counting rules, and the two-parton twist-3 contributions become leading-power in the B meson transition form factors [24]. This is our motivation to prove the corresponding factorization theorem. Note that the two-parton twist-3 contributions are next-to-leading-power in the pion form factor.

The momentum P_1 of the B meson and the momentum P_2 of the outgoing pion are parameterized as

$$P_1 = \frac{M_B}{\sqrt{2}}(1,1,\mathbf{0}_{\rm T}), \quad P_2 = \frac{M_B}{\sqrt{2}}(0,\eta,\mathbf{0}_{\rm T}), \quad (54)$$

where η denotes the energy fraction carried by the pion. Consider the kinematic region with small q^2, $q = P_1 - P_2$ being the lepton pair momentum, i.e., with large η, where PQCD is applicable. Let the light spectator $\bar{d}$ quark in the B meson (pion) carry the momentum k_1 ($k_2 = x_2P_2$), and the b quark carry the momentum $P_1 - k_1$. We have the equations of motion,

$$(\not{P}_1 - \not{k}_1 - m_b)b(P_1 - k_1) = 0, \quad \bar{d}(k_1)\not{k}_1 = 0, \quad (55)$$

where the $\bar{d}$ quark mass m_d has been neglected, and those for the valence quarks in the pion.

4.1 $O(\alpha_{\rm s})$ factorization

We start with the $O(\alpha_{\rm s})$ collinear factorization of the final-state distribution amplitudes. The lowest-order diagrams for the $B \to \pi l\nu$ decay are the same as in Fig. 1, but with the upper quark line in the initial state representing a b quark and with the symbol $\times$ representing a weak decay vertex. Figure 1a gives the amplitude,

$$G^{(0)}(x_1,x_2) = \frac{-g^2C_F}{2}\frac{u(\bar{x}_2P_2)\gamma^\nu(\not{P}_2 - \not{k}_1)\gamma_\mu b(P_1-k_1)}{(P_2-k_1)^2(k_1-x_2P_2)^2} \times \bar{d}(k_1)\gamma_\nu \bar{d}(x_2P_2). \quad (56)$$

Inserting the Fierz identity in (10) into the above expression, we obtain the trivial factorization formula,

$$G^{(0)}(x_1,x_2) = \int {\rm d}\xi_2 H_{\rm S}^{(0)}(x_1,\xi_2)\phi_{\rm S}^{(0)}(x_2,\xi_2), \quad (57)$$

with the lowest-order hard amplitude and distribution amplitude,

$$H_{\rm S}^{(0)}(x_1,\xi_2) = \frac{-g^2C_F}{2}m_0\frac{{\rm tr}[\gamma^\nu\not{P}_2\gamma_\mu b(P_1-k_1)\bar{d}(k_1)\gamma_\nu\gamma^5]}{(P_2-k_1)^2(k_1-x_2P_2+l)^2} = \frac{-g^2C_F}{2\eta^2M_B^4}m_0\frac{{\rm tr}[\gamma^\nu\not{P}_2\gamma_\mu b(P_1-k_1)\bar{d}(k_1)\gamma_\nu\gamma^5]}{x_1^2\xi_2},$$

$$\phi_{\rm S}^{(0)}(x_2,\xi_2) = \frac{1}{4m_0}u(\bar{x}_2P_2)\gamma_5 d(x_2P_2)\delta(\xi_2-x_2), \quad (58)$$

where the higher-power term $\not{k}_1$ in the numerator has been dropped. The PT structure does not contribute because of $\gamma^\nu(\not{n}_+\not{n}_- - 1)\gamma_5\gamma_\nu = 0$. It is observed that $H_{\rm S}^{(0)}$ depends only on the single plus component of k_1 through $k_1\cdot P_2$, which defines the momentum fraction $x_1 = k_1^+/P_1^+$ carried by the $\bar{d}$ quark in the B meson.

Consider $O(\alpha_{\rm s})$ corrections to Fig. 1a in the covariant gauge, which are displayed in Fig. 4 with the initial and final states being flipped. Here we summarize only the results of their factorization, and refer the details to Appendix C. The factorization of the two-particle reducible diagrams in Figs. 4a–c is straightforward. After inserting the Fierz identity, the loop integrals associated with Figs. 4a,b,c are written as

$$I^{(a),(b),(c)} \approx \int {\rm d}\xi_2 H_{\rm S}^{(0)}(x_1,\xi_2)\phi_{{\rm S}a,{\rm S}b,{\rm S}c}^{(1)}(x_2,\xi_2), \quad (59)$$

where the PS collinear pieces are given by

$$\phi_{{\rm S}a}^{(1)}(x_2,\xi_2) = \frac{-{\rm i}g^2C_F}{8m_0}\int\frac{{\rm d}^4l}{(2\pi)^4}u(\bar{x}_2P_2)\gamma_\beta\frac{\bar{x}_2\not{P}_2+\not{l}}{(\bar{x}_2P_2+l)^2}\gamma^\beta\frac{1}{\bar{x}_2\not{P}_2} \times\gamma_5 d(x_2P_2)\frac{1}{l^2}\delta(\xi_2-x_2), \quad (60)$$

$$\phi_{{\rm S}b}^{(1)}(x_2,\xi_2) = \frac{{\rm i}g^2C_F}{4m_0}\int\frac{{\rm d}^4l}{(2\pi)^4}u(\bar{x}_2P_2)\gamma_\beta\frac{\bar{x}_2\not{P}_2+\not{l}}{(\bar{x}_2P_2+l)^2}\gamma_5\frac{x_2\not{P}_2-\not{l}}{(x_2P_2-l)^2}$$

$$\times\gamma^\beta d(x_2P_2)\frac{1}{l^2}\delta\left(\xi_2-x_2+\frac{l^-}{P_2^-}\right), \tag{61}$$

$$\begin{aligned}\phi_{\mathrm{S}c}^{(1)}(x_2,\xi_2)&=\frac{-\mathrm{i}g^2C_F}{8m_0}\int\frac{\mathrm{d}^4l}{(2\pi)^4}u(\bar{x}_2P_2)\gamma_5\frac{1}{x_2\not{P}_2}\gamma_\beta\frac{x_2\not{P}_2-\not{l}}{(x_2P_2-l)^2}\\&\quad\times\gamma^\beta d(x_2P_2)\frac{1}{l^2}\delta(\xi_2-x_2)\,.\end{aligned} \tag{62}$$

The momentum fraction ξ_2 in Fig. 4b has been modified into $\xi_2=x_2-l^-/P_2^-$ by the collinear gluon exchange.

The collinear factorization of Figs. 4d–g is summarized as

$$\sum_{i=(d)}^{(g)}I^i\approx\int\mathrm{d}\xi_2H_{\mathrm{S}}^{(0)}(x_1,\xi_2)\phi_{\mathrm{S}u}^{(1)}(x_2,\xi_2)\,, \tag{63}$$

where the PS collinear piece,

$$\begin{aligned}\phi_{\mathrm{S}u}^{(1)}(x_2,\xi_2)=\frac{-\mathrm{i}g^2C_F}{4m_0}\int\frac{\mathrm{d}^4l}{(2\pi)^4}u(\bar{x}_2P_2)\gamma^\beta\frac{\bar{x}_2\not{P}_2+\not{l}}{(\bar{x}_2P_2+l)^2}\\\times\gamma_5 d(x_2P_2)\frac{1}{l^2}\frac{n_{+\beta}}{n_+\cdot l}\\\times\left[\delta(\xi_2-x_2)-\delta\left(\xi_2-x_2+\frac{l^-}{P_2^-}\right)\right],\end{aligned} \tag{64}$$

is associated with the collinear gluon emitted from the u quark. The appropriate color factor C_F indicates the factorization between the distribution amplitude and the hard amplitude in color space, which can be achieved only by summing a set of diagrams. The collinear divergent piece in (64) has been split into two terms as a consequence of the Ward identity. The first and second terms correspond to the cases without and with the loop momentum l flowing through the hard gluon, respectively. The Feynman rule $n_{+\beta}/n_+\cdot l$ in the collinear divergent pieces, coming from the eikonal approximation, can be represented by a Wilson line in the direction n_+.

The collinear factorization of Figs. 4h–k, derived in a similar way, is written as

$$\sum_{i=(h)}^{(k)}I^i\approx\int\mathrm{d}\xi_2H_{\mathrm{S}}^{(0)}(x_1,\xi_2)\phi_{\mathrm{S}\bar{d}}^{(1)}(x_2,\xi_2)\,, \tag{65}$$

where the PS piece,

$$\begin{aligned}\phi_{\mathrm{S}\bar{d}}^{(1)}(x_2,\xi_2)=\frac{\mathrm{i}g^2C_F}{4m_0}\int\frac{\mathrm{d}^4l}{(2\pi)^4}u(\bar{x}_2P_2)\gamma_5\frac{x_2\not{P}_2-\not{l}}{(x_2P_2-l)^2}\\\times\gamma^\beta d(x_2P_2)\frac{1}{l^2}\frac{n_{+\beta}}{n_+\cdot l}\\\times\left[\delta(\xi_2-x_2)-\delta\left(\xi_2-x_2+\frac{l^-}{P_2^-}\right)\right],\end{aligned} \tag{66}$$

is associated with the collinear gluon emitted from the $\bar{d}$ quark. Finally, the sum of (59), (63) and (65) gives

$$\sum_{i=(a)}^{(k)}I^i\approx\int\mathrm{d}\xi_2H_{\mathrm{S}}^{(0)}(x_1,\xi_2)\phi_{\mathrm{S}}^{(1)}(x_2,\xi_2)\,, \tag{67}$$

where the PS collinear piece $\phi_{\mathrm{S}}^{(1)}$ is defined by the $O(\alpha_{\mathrm{s}})$ term of the complex conjugate of (22), consistent with the universality.

The amplitude corresponding to Fig. 1b is written as

$$\begin{aligned}G^{(0)}(x_1,x_2)&=\frac{-g^2C_F}{2}\\&\quad\times\frac{u(\bar{x}_2P_2)\gamma_\mu(\not{P}_1-x_2\not{P}_2+m_b)}{[(P_1-x_2P_2)^2-m_b^2](k_1-x_2P_2)^2}\\&\quad\times\gamma^\nu b(P_1-k_1)\bar{d}(k_1)\gamma_\nu d(x_2P_2),\end{aligned} \tag{68}$$

which, after inserting the Fierz identity, leads to the trivial factorization formula,

$$G^{(0)}=\sum_{m=\mathrm{S,T}}\int\mathrm{d}\xi_2H_m^{(0)}(x_1,\xi_2)\phi_m^{(0)}(x_2,\xi_2)\,. \tag{69}$$

The lowest-order hard amplitudes and distribution amplitudes of the PS and PT structures are written as

$$\begin{aligned}H_{\mathrm{S}}^{(0)}(x_1,\xi_2)&=\frac{-g^2C_F}{2}m_0\\&\quad\times\frac{\mathrm{tr}[\gamma_\mu(\not{P}_1-\xi_2\not{P}_2+m_b)\gamma^\nu b(P_1-k_1)\bar{d}(k_1)\gamma_\nu\gamma_5]}{[(P_1-\xi_2P_2)^2-m_b^2](k_1-\xi_2P_2)^2}\\&=\frac{-g^2C_F}{2\eta^2M_B^4}m_0\\&\quad\times\frac{\mathrm{tr}[\gamma_\mu(\not{P}_1-\xi_2\not{P}_2+m_b)\gamma^\nu b(P_1-k_1)\bar{d}(k_1)\gamma_\nu\gamma_5]}{x_1\xi_2^2}\,,\\H_{\mathrm{T}}^{(0)}(x_1,\xi_2)&=\frac{-g^2C_F}{2}m_0\\&\quad\times\mathrm{tr}[\gamma_\mu(\not{P}_1-\xi_2\not{P}_2+m_b)\gamma^\nu b(P_1-k_1)\bar{d}(k_1)\\&\qquad\times\gamma_\nu(\not{n}_+\not{n}_--1)\gamma_5]\\&\quad/([(P_1-\xi_2P_2)^2-m_b^2](k_1-\xi_2P_2)^2)\,,\\\phi_{\mathrm{T}}^{(0)}(x_2,\xi_2)&=\frac{1}{4m_0}u(\bar{x}_2P_2)\gamma_5(\not{n}_+\not{n}_--1)d(x_2P_2)\delta(\xi_2-x_2)\,.\end{aligned} \tag{70}$$

The lowest-order PS distribution amplitude $\phi_{\mathrm{S}}^{(0)}(x_2,\xi_2)$ is the same as in (58).

Below we discuss the collinear divergences in the $O(\alpha_{\mathrm{s}})$ corrections to Fig. 1b, which are displayed in Fig. 2 with the initial states and the final states being flipped. The details are referred to Appendix C. Figures 2a–c are factorized straightforwardly, leading to

$$I^{(a),(b),(c)}\approx\sum_{m=\mathrm{S,T}}\int\mathrm{d}\xi_2H_m^{(0)}(x_1,\xi_2)\phi_{ma,mb,mc}^{(1)}(x_2,\xi_2)\,. \tag{71}$$

The PS collinear divergent functions $\phi^{(1)}_{Sa,Sb,Sc}(x_2,\xi_2)$ are the same as those shown in (60)–(62), respectively. The PT pieces have the similar expressions with γ_5 being replaced by γ_5 ($\not{n}_+$ $\not{n}_-$ − 1).

For the irreducible diagrams Figs. 2d–g, a summation of their contributions is necessary for obtaining the desired collinear factorization,

$$\sum_{i=(d)}^{(g)} I^i \approx \sum_{m=\mathrm{S,T}} \int \mathrm{d}\xi_2 H^{(0)}_m(x_1,\xi_2)\phi^{(1)}_{mu}(x_2,\xi_2)\,, \quad (72)$$

with the PS pieces $\phi^{(1)}_{Su}$ and $\phi^{(1)}_{S\bar{d}}$ shown in (64) and (66), respectively. The PT pieces have the similar expressions with γ_5 being replaced by γ_5 ($\not{n}_+$ $\not{n}_-$ − 1). The collinear factorization of Figs. 2h–k, derived in a similar way, is written as

$$\sum_{i=(h)}^{(k)} I^i \approx \sum_{m=\mathrm{S,T}} \int \mathrm{d}\xi_2 H^{(0)}_m(x_1,\xi_2)\phi^{(1)}_{m\bar{d}}(x_2,\xi_2)\,. \quad (73)$$

Finally, the sum of (71), (72) and (73) gives

$$\sum_{i=(a)}^{(k)} I^i \approx \sum_{m=\mathrm{S,T}} \int \mathrm{d}\xi_2 H^{(0)}_m(x_1,\xi_2)\phi^{(1)}_{m}(x_2,\xi_2)\,, \quad (74)$$

where the collinear divergent functions $\phi^{(1)}_m(x_2,\xi_2)$ are defined by the $O(\alpha_s)$ terms of the complex conjugate of (22).

The $O(\alpha_s)$ factorization of the soft divergences from the decay $B\to\pi l\nu$ has been performed in [1], which results in two B meson distribution amplitudes $\phi^{(1)}_+$ and $\phi^{(1)}_-$ [16,36] arising from the insertion of the fourth and fifth terms of the Fierz identity on the initial-state side:

$$\begin{aligned} I_{ij}I_{lk} = {} & \frac{1}{4}I_{ik}I_{lj} + \frac{1}{4}(\gamma_\alpha)_{ik}(\gamma^\alpha)_{lj} \\ & + \frac{1}{4}\left[\frac{1}{\sqrt{2}}\gamma_5(\not{v}-1)\right]_{ik}\left[\frac{1}{\sqrt{2}}(\not{v}-1)\gamma_5\right]_{lj} \\ & + \frac{1}{4}\left[\frac{1}{\sqrt{2}}\gamma_5\,\not{n}_+(\not{v}+1)\right]_{ik}\left[\frac{1}{\sqrt{2}}(\not{v}+1)\,\not{n}_-\gamma_5\right]_{lj} \\ & + \frac{1}{4}\left[\frac{1}{\sqrt{2}}\gamma_5\,\not{n}_-(\not{v}+1)\right]_{ik}\left[\frac{1}{\sqrt{2}}(\not{v}+1)\,\not{n}_+\gamma_5\right]_{lj}. \end{aligned} \quad (75)$$

The Wilson line on the light cone can be constructed, only if the hard scale for exclusive B meson decays is of $O(\sqrt{\bar{\Lambda}M_B})$. This Wilson line is crucial for the gauge-invariant definitions of the distribution amplitudes as non-local matrix elements.

Following the similar procedures in Sect. 2, we derive the $O(\alpha_s)$ factorization of the decay $B\to\pi l\nu$,

$$G^{(1)} = \sum_{n=+,-}\phi^{(1)}_n\otimes H^{(0)}_n + \sum_{m=\mathrm{S,T}} H^{(0)}_m\otimes\phi^{(1)}_m + H^{(1)}, \quad (76)$$

where the hard amplitude $H^{(0)}$ receives the contributions from Figs. 1a,b. Consequently, the factorization formula for the two-parton twist-3 contributions is written, up to $O(\alpha_s)$, as

$$\begin{aligned} & G^{(0)} + G^{(1)} \\ & = \sum_{\substack{n=+,-\\ m=\mathrm{S,T}}} (\phi^{(0)}_n + \phi^{(1)}_n)\otimes(H^{(0)}_{nm} + H^{(1)}_{nm})\otimes(\phi^{(0)}_m + \phi^{(1)}_m). \end{aligned} \quad (77)$$

The definitions for the hard amplitudes $H^{(1)}_{nm}$ and $H^{(0)}_{nm}$ are similar to those in (28). For example, the explicit expression of $H^{(0)}_{+S}$ is given by

$$\begin{aligned} & H^{(0)}_{+S}(\xi_1,\xi_2) \\ & = \frac{-g^2C_F}{2\sqrt{2}}m_0\left\{\frac{\mathrm{tr}[\gamma^\nu\ \not{P}_2\gamma_\mu(\not{P}_1+M_B)\ \not{n}_-\gamma_5\gamma_\nu\gamma_5]}{(P_2-k_1)^2(k_1-x_2P_2+l)^2}\right. \\ & \quad \left. + \frac{\mathrm{tr}[\gamma_\mu(\not{P}_1-\xi_2\ \not{P}_2+m_b)\gamma^\nu(\not{P}_1+M_B)\ \not{n}_-\gamma_5\gamma_\nu\gamma_5]}{[(P_1-\xi_2P_2)^2-m_b^2](k_1-\xi_2P_2)^2}\right\}. \end{aligned} \quad (78)$$

4.2 All-order factorization

The all-order proof of the two-parton twist-3 factorization theorem for the process $\pi\gamma^*\to\pi$ in Sect. 3 can be generalized to the $B\to\pi l\nu$ decay with minor modifications. Here we highlight only the different points of the proof. In the case of B meson decays there is no collinear divergence associated with the initial state, since the b quark is massive, and the light spectator $\bar{d}$ quark is soft [1]. Hence, the B meson side is dominated by the soft divergence. The collinear configurations associated with the final-state pion are the same as in the process $\pi\gamma^*\to\pi$ discussed in Sect. 2. The important infrared divergences are then classified into the soft type with a small loop momentum l and the collinear type with l parallel to P_2. We shall compare the factorizations of the soft divergences into the initial state and of the collinear divergences into the final state.

Identify the soft gluon emitted from the outer most vertex α on the b quark line in the $O(\alpha_s^{N+1})$ diagrams $G^{(N+1)}$. Let β denote the attachments of the other end of the identified gluon inside the diagrams. The attachments of the soft gluon to collinear lines along P_2, to soft lines, and to hard lines along P_2-k_1 all give soft divergences. The soft lines include the b quark line, the spectator $\bar{d}$ quark line, and soft internal lines. The hard lines in exclusive B meson decays are off-shell only by $O((P_2-k_1)^2)\sim O(\bar{\Lambda}M_B)$ [1]. When the identified gluon attaches the collinear lines along P_2 and the hard lines, the vertex β inside the diagrams is mainly minus, and the vertex α on the b quark line is mainly plus. The corresponding soft divergences are classified as the first type, and the replacement in (37) holds for their factorization. The above observations hint to a modified decomposition of the tensor $g_{\alpha\beta}$ for the identified gluon,

$$\begin{aligned} g_{\alpha\beta} = {} & \frac{n_{-\alpha}l_\beta}{n_-\cdot l} - \delta_{\alpha\perp}\delta_{\beta\perp} + \left(\delta_{\alpha+}\delta_{\beta-} - \frac{n_{-\alpha}l_\beta}{n_-\cdot l}\right) \\ & + \delta_{\alpha-}\delta_{\beta+}\,. \end{aligned} \quad (79)$$

The second term in (79) does not lead to soft divergences due to the equations of motion. For the third and fourth terms, the identified gluon attaches only the soft lines, leading to the second type of soft divergences. Similarly, this type of divergences is included by recovering the Lorentz covariance of the factorization. For the identified soft gluon emitted by the spectator $\bar{d}$ quark, the decomposition in (79) also works. The differences are that the second and third terms give the second type of soft divergences, and that the fourth term does not contribute because of the equations of motion.

Since the collinear configurations for the final-state side are the same as those in the process $\pi\gamma^* \to \pi$, (39) holds. The difference between the factorizations of the soft divergences into the initial state and of the collinear divergences into the final state is then clear. Based on the above discussion, the factorization of the $O(\alpha_{\rm s}^{(N+1)})$ diagrams $G^{(N+1)}$ follows exactly the same induction procedure in Sect. 3. In this case, the subscript n for the B meson distribution amplitudes denotes $n = +, -$. We then obtain the factorization formula,

$$G^{(N+1)} = \sum_{\substack{n=+,-\\ m=\mathrm{S,T}}} \sum_{i=0}^{N+1} \sum_{j=0}^{N+1-i} \phi_n^{(i)} \otimes H_{nm}^{(N+1-i-j)} \otimes \phi_m^{(j)}, \quad (80)$$

where the $O(\alpha_{\rm s}^{N+1})$ hard amplitude $H_{nm}^{(N+1)}$ is infrared finite. Equation (80) indicates that all the soft and collinear divergences in the semileptonic decay $B \to \pi l\nu$ can be factorized into the distribution amplitudes $\phi_n^{(i)}$ and $\phi_m^{(j)}$ at the parton level order by order, and that the proof of the corresponding two-parton twist-3 factorization theorem is completed. These parton-level distribution amplitudes serve as the infrared regulators for the derivation of the hard amplitudes from the parton-level diagrams.

To compute the $B \to \pi$ transition form factor, we convolute the hard amplitudes with the meson distribution amplitudes, in which the quark states are replaced by the physical B meson and pion states. Both the twist-2 and two-parton twist-3 contributions to the $B \to \pi$ form factors $F_+(q^2)$ and $F_0(q^2)$ in the standard definition have been evaluated in [24]. It was observed that the latter are of the same order of magnitude as the former, consistent with the argument that the two-parton twist-3 contributions are not power-suppressed and are chirally enhanced. The light-cone sum rules also give approximately equal weights to the twist-2 and two-parton twist-3 contributions to F_+ [37].

5 Conclusion

In this paper we have investigated the infrared divergences in the process $\pi\gamma^* \to \pi$ at the two-parton twist-3 level. We summarize our observations below. There are no soft divergences associated with the pion, since they cancel among diagrams. The absence of the soft divergences is related to the fact that a soft gluon, being huge in space-time, does not resolve the color structure of the color-singlet pion. In the collinear region with the loop momentum parallel to the pion momentum, we have shown that the delicate summation of many diagrams leads to the $O(\alpha_{\rm s})$ factorization in the momentum, spin and color spaces. We have presented an all-order proof of the two-parton twist-3 factorization theorem for the process $\pi\gamma^* \to \pi$ by means of the Ward identity. This proof can also accommodate the twist-2 factorization theorem presented in [1] and the twist-4 one simply by considering the corresponding structures in the Fierz transformation in (10).

The idea of the proof is to decompose the tensor $g_{\alpha\beta}$ for the identified collinear gluon into the longitudinal and transverse pieces shown in (36). The longitudinal (transverse) piece corresponds to the configuration without (with) the attachment of the identified gluon to a line along the external momentum. The former configuration can be factorized using the Ward identity as hinted by the replacement in (37). The factorization of the latter configuration can be included by demanding the Lorentz covariance of the factorization. We emphasize again that the parton-level distribution amplitudes, similar to the effective diagrams drawn in SCET [26, 27], serve as the infrared regulators for the derivation of the hard amplitudes from the parton-level diagrams. The hard amplitudes are then derived from the "matching procedure". Based on the perturbative construction of the distribution amplitudes, we have derived their two-parton twist-3 definitions as non-local matrix elements, where the path-ordered Wilson line appears as a consequence of the Ward identity. Note that our technique is simple compared to that based on the "Δ-forest" prescription in [5], and explicitly gauge invariant compared to that performed in the axial gauge [2].

We have generalized the proof to the more complicated semileptonic decay $B \to \pi l\nu$. The collinear factorization for the final-state pion is the same as in the process $\pi\gamma^* \to \pi$. The identical collinear structures in both processes justify the concept of universality of hadron distribution amplitudes in PQCD. The factorization of the soft divergences for the initial-state B meson has been discussed in [1]. The conceptual differences are summarized as follows. The decomposition of the tensor $g_{\alpha\beta}$ for the identified soft gluon in (36) and the replacement in (37) still work. However, the correspondence between each term in the decomposition and the type of soft divergences changes, as explained after (79). The procedures of the proof then follow those for the pion form factor. The attachments of a soft gluon to the hard lines off-shell by $O(\bar{\Lambda}M_B)$ lead to soft divergences. These divergences, like those from the attachments of a collinear gluon to the hard lines in the process $\pi\gamma^* \to \pi$, are crucial for constructing the Wilson line, that guarantees the gauge invariance of the B meson distribution amplitudes. This explains why the characteristic scale of exclusive B meson decays, if factorizable, must be of $O(\bar{\Lambda}M_B)$.

For a practical application to the $B \to \pi l\nu$ decay, the parton transverse momenta $k_{\rm T}$ must be taken into account in order to smear the end-point singularities in the hard amplitudes [24, 38]. This observation implies the necessity of proving the $k_{\rm T}$ factorization theorem [17, 18]. The proof of the $k_{\rm T}$ factorization theorem is basically the same as proposed in this paper: we simply retain the dependence on

the loop transverse momenta in hard amplitudes [19]. The relative importance of the twist-2 and two-parton twist-3 contributions to the $B \to \pi$ transition form factor has been investigated in [24], which confirms our motivation to prove the two-parton twist-3 factorization theorem: the latter contributions are not power-suppressed and are chirally enhanced. In a future work the proof will be generalized to non-leptonic B meson decays, such as $B \to K\pi$ and $\pi\pi$ [39, 40]. The corresponding factorization theorem is much more complicated, since non-leptonic decays involve three characteristic scales: the W boson mass M_W, M_B, and the hadronic scale of $O(\bar{\Lambda})$, such as the parton transverse momenta $k_{\rm T}$ [41, 42].

Finally, we compare our construction of the collinear factorization theorem in perturbation theory with that in SCET. In the former one starts with Feynman diagrams in full QCD. Look for the leading region of the loop momentum defined by (4), in which one makes the power counting of the Feynman diagrams. It can be found that the approximate loop integral in the leading region is represented by the diagram in Fig. 3e, which leads to the definition of a distribution amplitude. In SCET one first constructs the various effective degrees of freedom describing infrared dynamics and the effective interactions, and defines their powers. Select a specific effective operator, such as those non-local operators in (3). Draw the diagrams based on the effective theory, and then make the power counting. It can be shown that the diagram in Fig. 3e scales like the selected operator, and builds up the distribution amplitude. It is not necessary to analyze the infrared divergences in diagrams at this stage. That is, one arrives at Fig. 3e through approximating loop integrals in the full theory in PQCD, but does at the operator and Lagrange level in SCET. Despite of the different reasonings for deriving a collinear factorization formula, the calculation of the Wilson coefficients is the same. As calculating the Wilson coefficients associated with the effective operators from the matching procedure in SCET, the infrared divergences need to be analyzed, and their cancellation between the full theory and the effective theory must be demonstrated explicitly. This procedure is in fact the same as the derivation of the hard amplitudes (Wilson coefficients) in PQCD, where the subtraction of the distribution amplitudes (the effective theory) from the parton-level diagrams (the full theory) is done. Therefore, it is legitimate to claim that the constructions of the collinear factorization theorem are equivalent between PQCD and SCET [29].

Acknowledgements. We thank S. Brodsky, A.I. Sanda, and G. Sterman for useful discussions. This work was supported in part by the National Science Council of R.O.C. under the Grant No. NSC-92-2112-M-001-030, by National Center for Theoretical Sciences of R.O.C., and by Grant-in Aid for Special Project Research (Physics of CP Violation) from the Ministry of Education, Science and Culture, Japan.

Appendix A: $O(\alpha_{\rm s})$ corrections from Fig. 2

In this appendix we demonstrate the $O(\alpha_{\rm s})$ factorization at the twist-3 level of Fig. 2 in the collinear configuration. The collinear divergences associated with the additional gluon carrying the momentum l parallel to P_1 will be grouped into the initial-state pion distribution amplitude. It is obvious that the twist-2 collinear factorization is performed in the same way. Since the factorizations of Figs. 2a,c are similar to that of Fig. 2b, we present the details only for Figs. 2b and 2(d)-2(k).

The loop integral of Fig. 2b is given by

$$\begin{aligned} I^{(b)} & \qquad\qquad (A.1) \\ = & \frac{-eg^4C_F^2}{2}\int\frac{\mathrm{d}^4 l}{(2\pi)^4}\left[\bar{d}(x_1P_1)\gamma_\beta\frac{x_1\not{P}_1-\not{l}}{(x_1P_1-l)^2}\right]_i (I)_{ij} \\ & \times\left[\gamma_\alpha d(x_2P_2)\bar{u}(\bar{x}_2P_2)\gamma^\alpha\frac{\not{P}_2-x_1\not{P}_1+\not{l}}{(P_2-x_1P_1+l)^2}\gamma_\mu\right]_{jl}(I)_{lk} \\ & \times\left[\frac{\bar{x}_1\not{P}_1+\not{l}}{(\bar{x}_1P_1+l)^2}\gamma^\beta u(\bar{x}_1P_1)\right]_k \frac{1}{l^2(x_2P_2-x_1P_1+l)^2}\,, \end{aligned}$$

where we have introduced the identity matrices, $(I)_{ij}$ and $(I)_{lk}$, in order to make explicit the positions of inserting the Fierz identity. With (10), focusing on the twist-3 structures, we obtain

$$\begin{aligned} I^{(b)} \approx & \frac{\mathrm{i}g^2C_F}{4m_0}\int\frac{\mathrm{d}^4 l}{(2\pi)^4}\bar{d}(x_1P_1)\gamma_\beta\frac{x_1\not{P}_1-\not{l}}{(x_1P_1-l)^2} \\ & \times\gamma_5\frac{\bar{x}_1\not{P}_1+\not{l}}{(\bar{x}_1P_1+l)^2}\gamma^\beta u(\bar{x}_1P_1)\frac{1}{l^2} \\ & \times\frac{\mathrm{i}}{2}eg^2C_Fm_0 \\ & \times\mathrm{tr}[\gamma_\alpha\bar{d}(x_2P_2)u(\bar{x}_2P_2) \\ & \qquad \gamma^\alpha(\not{P}_2-x_1\not{P}_1+\not{l})\gamma_\mu\gamma_5] \\ & /((P_2-x_1P_1+l)^2(x_2P_2-x_1P_1+l)^2) \\ & +\frac{\mathrm{i}g^2C_F}{4m_0}\int\frac{\mathrm{d}^4 l}{(2\pi)^4}\bar{d}(x_1P_1)\gamma_\beta\frac{x_1\not{P}_1-\not{l}}{(x_1P_1-l)^2} \\ & \times\gamma_5(\not{n}_+\not{n}_--1)\frac{\bar{x}_1\not{P}_1+\not{l}}{(\bar{x}_1P_1+l)^2}\gamma^\beta u(\bar{x}_1P_1)\frac{1}{l^2} \\ & \times\frac{\mathrm{i}}{2}eg^2C_Fm_0 \\ & \times\mathrm{tr}\left[\gamma_\alpha\bar{d}(x_2P_2)u(\bar{x}_2P_2)\gamma^\alpha(\not{P}_2-x_1\not{P}_1+\not{l})\right. \\ & \qquad \left.\times\gamma_\mu(\not{n}_+\not{n}_--1)\gamma_5\right] \\ & /((P_2-x_1P_1+l)^2(x_2P_2-x_1P_1+l)^2)\,, \qquad (A.2) \end{aligned}$$

where the twist-2 structure $(\gamma_5\not{n}_-)_{ik}(\not{n}_+\gamma_5)_{jl}$ has been dropped. In the collinear region with $l \parallel P_1$, the dependence on l^- and on $l_{\rm T}$ in (A.2), being subleading according to (4), needs to be neglected. Inserting the identity $\int\mathrm{d}\xi_1\delta(\xi_1-x_1+l^+/P_1^+)=1$, the first factors of the above two terms on the right-hand side of (A.2) give the collinear

divergent piece $\phi^{(1)}_{\mathrm{S(T)}b}(x_1,\xi_1)$ defined in (15). The second factors are the corresponding hard amplitude $H^{(0)}_{\mathrm{S(T)}}(\xi_1,x_2)$ defined in (12).

For the loop integrals associated with the two-particle irreducible diagrams in Figs. 2d–k, the collinear factorization is a bit complicated. It will be shown, with the Ward identity, that the sum of Figs. 2d–g and the sum of Figs. 2h–k lead to the factorization formulas in (17) and (19) with the collinear divergent pieces being defined by $\phi^{(1)}_{\mathrm{S(T)}u}(x_1,\xi_1)$ and $\phi^{(1)}_{\mathrm{S(T)}\bar{d}}(x_1,\xi_1)$, respectively. Start from Fig. 2d, whose loop integral is written as

$$\begin{aligned} I^{(d)} = {} & \frac{\mathrm{i}eg^4}{2N_c}\int\frac{\mathrm{d}^4l}{(2\pi)^4}\,\bar{d}(x_1P_1)\gamma^\lambda d(x_2P_2)\bar{u}(\bar{x}_2P_2) \\ & \times\gamma^\beta\frac{\not P_2-x_1\not P_1+\not l}{(P_2-x_1P_1+l)^2}\gamma_\mu\frac{\bar{x}_1\not P_1+\not l}{(\bar{x}_1P_1+l)^2} \\ & \times\gamma^\alpha u(\bar{x}_1P_1)\frac{\mathrm{tr}(T^cT^bT^a)\Gamma^{cba}_{\lambda\beta\alpha}}{l^2(x_1P_1-x_2P_2)^2(x_1P_1-x_2P_2-l)^2}\,, \end{aligned} \tag{A.3}$$

with the number of colors $N_c=3$, the color matrices $T^{a(b,c)}$ and the triple-gluon vertex,

$$\begin{aligned} \Gamma^{cba}_{\lambda\beta\alpha} = {} & f^{cba}[g_{\alpha\beta}(2l-x_1P_1+x_2P_2)_\lambda \\ & +g_{\beta\lambda}(2x_1P_1-2x_2P_2-l)_\alpha \\ & +g_{\lambda\alpha}(x_2P_2-x_1P_1-l)_\beta]\,, \end{aligned} \tag{A.4}$$

where f^{abc} is an antisymmetric tensor. The above color structure can be simplified by employing the identities,

$$\begin{aligned} & \mathrm{tr}(T^aT^bT^c)=\frac{1}{4}(d^{abc}+\mathrm{i}f^{abc})\,,\quad d^{abc}f^{abc}=0\,, \\ & f^{abc}f^{abc}=24\,, \end{aligned} \tag{A.5}$$

d^{abc} being a symmetric tensor. By means of the equations of motion in (9), γ^α sandwiched between $\bar{x}_1\not P_1+\not l$ and $u(\bar{x}_1P_1)$ must be γ^+, and γ^λ sandwiched between $\bar{d}(x_1P_1)$ and $d(x_2P_2)$ must be γ_T in the collinear region with $l\parallel P_1$. Therefore, only the second term $g_{\beta\lambda}(-2x_2P_{2\alpha})$ contributes at leading level, and the terms proportional to $g_{\alpha\beta}(2l_\mathrm{T})$ and to $g_{\lambda\alpha}$ are suppressed at least by $O(\lambda/Q)$.

For the leading term, we have the following approximation,

$$\begin{aligned} & \frac{2x_2P_{2\alpha}}{(x_1P_1-x_2P_2)^2(x_1P_1-x_2P_2-l)^2} \\ & \approx\frac{n_{-\alpha}}{n_-\cdot l}\left[\frac{1}{(x_1P_1-x_2P_2)^2}-\frac{1}{(x_1P_1-x_2P_2-l)^2}\right], \end{aligned} \tag{A.6}$$

and the eikonal propagator appears as a consequence of the splitting of the hard gluon propagators. Equation (A.6) is an example of the Ward identity [1]. Accordingly, (A.3) becomes

$$\begin{aligned} I^{(d)} = {} & eg^4\int\frac{\mathrm{d}^4l}{(2\pi)^4}\bar{d}(x_1P_1)\gamma_\beta d(x_2P_2)\bar{u}(\bar{x}_2P_2)\gamma^\beta \\ & \times\frac{\not P_2-x_1\not P_1+\not l}{(P_2-x_1P_1+l)^2}\gamma_\mu \\ & \times\frac{\bar{x}_1\not P_1+\not l}{(\bar{x}_1P_1+l)^2}\gamma^\alpha u(\bar{x}_1P_1)\,\frac{1}{l^2}\,\frac{n_{-\alpha}}{n_-\cdot l} \\ & \times\left[\frac{1}{(x_1P_1-x_2P_2)^2}-\frac{1}{(x_1P_1-x_2P_2-l)^2}\right]. \end{aligned} \tag{A.7}$$

The loop integrals associated with Figs. 2e,f are given by

$$\begin{aligned} I^{(e)} = {} & \frac{-eg^4C_F}{4N_c}\int\frac{\mathrm{d}^4l}{(2\pi)^4}\,\bar{d}(x_1P_1)\gamma_\alpha d(x_2P_2)\bar{u}(\bar{x}_2P_2) \\ & \times\gamma_\beta\frac{\bar{x}_2\not P_2+\not l}{(\bar{x}_2P_2+l)^2}\gamma^\alpha\frac{\not P_2-x_1\not P_1+\not l}{(P_2-x_1P_1+l)^2}\gamma_\mu \\ & \times\frac{\bar{x}_1\not P_1+\not l}{(\bar{x}_1P_1+l)^2}\gamma^\beta u(\bar{x}_1P_1)\frac{1}{l^2(x_1P_1-x_2P_2)^2}\,, \\ I^{(f)} = {} & \frac{eg^4C_F}{4N_c}\int\frac{\mathrm{d}^4l}{(2\pi)^4}\,\bar{d}(x_1P_1)\gamma^\alpha\frac{x_2\not P_2+\not l}{(x_2P_2+l)^2} \\ & \times\gamma_\beta d(x_2P_2)\bar{u}(\bar{x}_2P_2)\gamma_\alpha\frac{\not P_2-x_1\not P_1+\not l}{(P_2-x_1P_1+l)^2}\gamma_\mu \\ & \times\frac{\bar{x}_1\not P_1+\not l}{(\bar{x}_1P_1+l)^2}\gamma^\beta u(\bar{x}_1P_1)\frac{1}{l^2(x_1P_1-x_2P_2-l)^2}\,, \end{aligned} \tag{A.8}$$

respectively. In the collinear configuration $\gamma^\beta(\gamma_\beta)$ must be $\gamma^+(\gamma^-)$, and we apply the eikonal approximations,

$$\begin{aligned} & \bar{u}(\bar{x}_2P_2)\gamma_\beta\frac{\bar{x}_2\not P_2+\not l}{(\bar{x}_2P_2+l)^2}\approx\bar{u}(\bar{x}_2P_2)\frac{n_{-\beta}}{n_-\cdot l}\,, \\ & \frac{x_2\not P_2+\not l}{(x_2P_2+l)^2}\gamma_\beta\,d(x_2P_2)\approx\frac{n_{-\beta}}{n_-\cdot l}d(x_2P_2)\,. \end{aligned} \tag{A.9}$$

Combining the loop integrals in (A.8), we obtain an expression similar to (A.7) but with a different color factor,

$$\begin{aligned} I^{(e)}+I^{(f)} = {} & \frac{-eg^4C_F}{4N_c}\int\frac{\mathrm{d}^4l}{(2\pi)^4}\bar{d}(x_1P_1)\gamma_\alpha d(x_2P_2)\bar{u}(\bar{x}_2P_2) \\ & \times\gamma^\alpha\frac{\not P_2-x_1\not P_1+\not l}{(P_2-x_1P_1+l)^2}\gamma_\mu \\ & \times\frac{\bar{x}_1\not P_1+\not l}{(\bar{x}_1P_1+l)^2}\gamma^\beta u(\bar{x}_1P_1)\,\frac{1}{l^2}\,\frac{n_{-\beta}}{n_-\cdot l} \\ & \times\left[\frac{1}{(x_1P_1-x_2P_2)^2}-\frac{1}{(x_1P_1-x_2P_2-l)^2}\right]. \end{aligned} \tag{A.10}$$

Note that there has not yet been a consistent loop momentum flow between the hard fermion propagators in the first lines of (A.7) and (A.10) and the hard gluon propagators in the second lines. There should exist l-independent hard fermion propagators corresponding to the first l-independent hard gluon propagators in the second lines. To arrive at a desired factorization form, the collinear divergence in Fig. 2g has to be included. The integral of Fig. 2g is written as

$$I^{(g)} = \frac{eg^4C_F^2}{2}\int\frac{\mathrm{d}^4l}{(2\pi)^4}\bar{d}(x_1P_1)$$

$$\times\gamma_\alpha d(x_2P_2)\bar{u}(\bar{x}_2P_2)\gamma^\alpha\frac{\not P_2-x_1\not P_1}{(P_2-x_1P_1)^2}$$
$$\times\gamma_\beta\frac{\not P_2-x_1\not P_1+\not l}{(P_2-x_1P_1+l)^2}\gamma_\mu \tag{A.11}$$
$$\times\frac{\bar{x}_1\not P_1+\not l}{(\bar{x}_1P_1+l)^2}\gamma^\beta u\,(\bar{x}_1P_1)\frac{1}{l^2(x_1P_1-x_2P_2)^2}\,.$$

In the collinear region with $l\parallel P_1$ the leading contribution comes from $\gamma^\beta(\gamma_\beta)=\gamma^+(\gamma^-)$, and the two internal fermion propagators sandwiching γ_β can be approximated by

$$\frac{\not P_2-x_1\not P_1}{(P_2-x_1P_1)^2}\gamma_\beta\frac{\not P_2-x_1\not P_1+\not l}{(P_2-x_1P_1+l)^2} \tag{A.12}$$
$$=\frac{n_{-\beta}}{n_-\cdot l}\left[\frac{\not P_2-x_1\not P_1}{(P_2-x_1P_1)^2}-\frac{\not P_2-x_1\not P_1+\not l}{(P_2-x_1P_1+l)^2}\right].$$

The loop integral $I^{(g)}$ is then simplified into

$$I^{(g)}\approx\frac{eg^4C_F^2}{2}\int\frac{\mathrm{d}^4l}{(2\pi)^4}\bar{d}(x_1P_1)\gamma_\alpha d(x_2P_2)\bar{u}(\bar{x}_2P_2) \tag{A.13}$$
$$\times\gamma^\alpha\left(\frac{\not P_2-x_1\not P_1}{(P_2-x_1P_1)^2}-\frac{\not P_2-x_1\not P_1+\not l}{(P_2-x_1P_1+l)^2}\right)\gamma_\mu$$
$$\times\frac{\bar{x}_1\not P_1+\not l}{(\bar{x}_1P_1+l)^2}\gamma^\beta u\,(\bar{x}_1P_1)\frac{1}{l^2}\frac{n_{-\beta}}{n_-\cdot l}\frac{1}{(x_1P_1-x_2P_2)^2}\,.$$

Summing (A.7), (A.10) and (A.13), we have

$$\sum_{i=(d)}^{(g)}I^i=\frac{eg^4C_F^2}{2}\int\frac{\mathrm{d}^4l}{(2\pi)^4}\bar{d}(x_1P_1)\gamma_\alpha d(x_2P_2)\bar{u}(\bar{x}_2P_2)$$
$$\times\gamma^\alpha\frac{\not P_2-x_1\not P_1}{(P_2-x_1P_1)^2}\gamma_\mu$$
$$\times\frac{\bar{x}_1\not P_1+\not l}{(\bar{x}_1P_1+l)^2}\gamma^\beta u(\bar{x}_1P_1)\;\frac{1}{l^2}\frac{n_{-\beta}}{n_-\cdot l}\frac{1}{(x_1P_1-x_2P_2)^2}$$
$$-\frac{eg^4C_F^2}{2}\int\frac{\mathrm{d}^4l}{(2\pi)^4}\bar{d}(x_1P_1)\gamma_\alpha d(x_2P_2)\bar{u}(\bar{x}_2P_2)$$
$$\times\gamma^\alpha\frac{\not P_2-x_1\not P_1+\not l}{(P_2-x_1P_1+l)^2}\gamma_\mu \tag{A.14}$$
$$\times\frac{\bar{x}_1\not P_1+\not l}{(\bar{x}_1P_1+l)^2}\gamma^\beta u(\bar{x}_1P_1)\;\frac{1}{l^2}\frac{n_{-\beta}}{n_-\cdot l}\frac{1}{(x_1P_1-x_2P_2-l)^2}\,,$$

in which both terms exhibit consistent loop momentum flows. The first term, where the internal particles are free from the l dependence, corresponds to the case without the loop momentum flowing through the hard amplitude. The second term corresponds to the case with the loop momentum flowing through the hard amplitude. Inserting the Fierz identity at the appropriate positions, we obtain (17) with the collinear divergent piece being defined by (18). The absence of the soft divergences is obvious from the cancellation in the loop integral of Fig. 2d, in the loop integral of Fig. 2g, and between the integrals of Figs. 2e,f as $l\to 0$.

The factorization formula in (19) can be derived in the similar way. Figure 2h gives the loop integral,

$$I^{(h)}=\frac{-ieg^4}{2N_c}\int\frac{\mathrm{d}^4l}{(2\pi)^4}\bar{d}(x_1P_1)\gamma^\lambda\frac{x_1\not P_1-\not l}{(x_1P_1-l)^2}$$
$$\times\gamma^\beta d(x_2P_2)\bar{u}(\bar{x}_2P_2)\gamma^\alpha\frac{\not P_2-x_1\not P_1}{(P_2-x_1P_1)^2} \tag{A.15}$$
$$\times\gamma_\mu u(\bar{x}_1P_1)\frac{\mathrm{tr}(T^cT^bT^a)\Gamma^{cba}_{\lambda\beta\alpha}}{l^2(x_1P_1-x_2P_2-l)^2(x_1P_1-x_2P_2)^2}\,,$$

with the triple-gluon vertex,

$$\Gamma^{cba}_{\lambda\beta\alpha}=f^{cba}[g_{\beta\lambda}(2l-x_1P_1+x_2P_2)_\alpha$$
$$+g_{\alpha\beta}(2x_1P_1-2x_2P_2-l)_\lambda$$
$$+g_{\lambda\alpha}(x_2P_2-x_1P_1-l)_\beta]\,. \tag{A.16}$$

By means of the equations of motion, it is shown that only the term $g_{\alpha\beta}(-2x_2P_{2\lambda})$ contains the collinear divergence based on the similar reasoning applied to Fig. 2d. Using (A.6), (A.15) becomes

$$I^{(h)}=-eg^4\int\frac{\mathrm{d}^4l}{(2\pi)^4}\bar{d}(x_1P_1)\gamma^\lambda\frac{x_1\not P_1-\not l}{(x_1P_1-l)^2}$$
$$\times\gamma_\alpha d(x_2P_2)\bar{u}(\bar{x}_2P_2)\gamma^\alpha\frac{\not P_2-x_1\not P_1}{(P_2-x_1P_1)^2}\gamma_\mu$$
$$\times u(\bar{x}_1P_1)\frac{1}{l^2}\frac{n_{-\lambda}}{n_-\cdot l} \tag{A.17}$$
$$\times\left[\frac{1}{(x_1P_1-x_2P_2)^2}-\frac{1}{(x_1P_1-x_2P_2-l)^2}\right].$$

The loop integrals associated with Figs. 2i,j are written as

$$I^{(i)}=\frac{-eg^4C_F}{4N_c}\int\frac{\mathrm{d}^4l}{(2\pi)^4}\bar{d}(x_1P_1)\gamma^\beta\frac{x_1\not P_1-\not l}{(x_1P_1-l)^2}$$
$$\times\gamma^\alpha\frac{x_2\not P_2-\not l}{(x_2P_2-l)^2}\gamma_\beta d(x_2P_2)\bar{u}(\bar{x}_2P_2)\gamma_\alpha\frac{\not P_2-x_1\not P_1}{(P_2-x_1P_1)^2}$$
$$\times\gamma_\mu u(\bar{x}_1P_1)\frac{1}{l^2(x_1P_1-x_2P_2)^2}\,,$$
$$I^{(j)}=\frac{eg^4C_F}{4N_c}\int\frac{\mathrm{d}^4l}{(2\pi)^4}\bar{d}(x_1P_1)\gamma^\beta\frac{x_1\not P_1-\not l}{(x_1P_1-l)^2}$$
$$\times\gamma^\alpha d(x_2P_2)\bar{u}(\bar{x}_2P_2)\gamma_\beta\frac{\bar{x}_2\not P_2-\not l}{(\bar{x}_2P_2-l)^2} \tag{A.18}$$
$$\times\gamma_\alpha\frac{\not P_2-x_1\not P_1}{(P_2-x_1P_1)^2}\gamma_\mu u(\bar{x}_1P_1)\frac{1}{l^2(x_1P_1-x_2P_2-l)^2}\,.$$

Employing the same eikonal approximation as in (A.9), we derive the simplified combination,

$$I^{(i)}+I^{(j)}$$
$$\approx\frac{eg^4C_F}{4N_c}\int\frac{\mathrm{d}^4l}{(2\pi)^4}\bar{d}(x_1P_1)$$

$$\times\gamma^\beta \frac{x_1\ \not{P}_1 - \not{l}}{(x_1P_1-l)^2}\gamma^\alpha d(x_2P_2)\bar{u}(\bar{x}_2P_2)$$
$$\times\gamma_\alpha \frac{\not{P}_2 - x_1\ \not{P}_1}{(P_2-x_1P_1)^2}\gamma_\mu u(\bar{x}_1P_1)\frac{1}{l^2}\frac{n_{-\beta}}{n_-\cdot l} \qquad (A.19)$$
$$\times\left[\frac{1}{(x_1P_1-x_2P_2)^2}-\frac{1}{(x_1P_1-x_2P_2-l)^2}\right].$$

Again, (A.17) and (A.19) have not yet been in the expected factorization form, and the contribution from Fig. 2k needs to be taken into account.

Finally, the integral associated with Fig. 2k is written as

$$I^{(k)} = \frac{-eg^4C_F^2}{2}\int\frac{\mathrm{d}^4l}{(2\pi)^4}\bar{d}(x_1P_1)\gamma^\beta\frac{x_1\ \not{P}_1 - \not{l}}{(x_1P_1-l)^2} \qquad (A.20)$$
$$\times\gamma^\alpha d(x_2P_2)\bar{u}(\bar{x}_2P_2)\gamma_\alpha\frac{\not{P}_2 - x_1\ \not{P}_1 + \not{l}}{(P_2-x_1P_1+l)^2}\gamma_\beta$$
$$\times\frac{\not{P}_2 - x_1\ \not{P}_1}{(P_2-x_1P_1)^2}\gamma_\mu u(\bar{x}_1P_1)\frac{1}{l^2(x_1P_1-x_2P_2-l)^2}.$$

Based on the similar reasoning applied to (A.11), the leading contribution comes from $\gamma^\beta(\gamma_\beta)=\gamma^+(\gamma^-)$, and (A.12) holds. We then have

$$I^{(k)} = \frac{-eg^4C_F^2}{2}\int\frac{\mathrm{d}^4l}{(2\pi)^4}\bar{d}(x_1P_1) \qquad (A.21)$$
$$\times\gamma^\beta\frac{x_1\ \not{P}_1 - \not{l}}{(x_1P_1-l)^2}\gamma^\alpha d(x_2P_2)\bar{u}(\bar{x}_2P_2)$$
$$\times\gamma_\alpha\left(\frac{\not{P}_2 - x_1\ \not{P}_1}{(P_2-x_1P_1)^2}-\frac{\not{P}_2 - x_1\ \not{P}_1 + \not{l}}{(P_2-x_1P_1+l)^2}\right)\gamma_\mu$$
$$\times u(\bar{x}_1P_1)\frac{1}{l^2}\frac{n_{-\beta}}{n_-\cdot l}\frac{1}{(x_1P_1-x_2P_2-l)^2}.$$

Combining (A.17), (A.19) and (A.21), and inserting the Fierz identity, we finally arrive at (19) with the collinear divergent piece being defined by (20). Similarly, the soft divergences cancel in the loop integral of Fig. 2h, in the loop integral of Fig. 2k, and between the integrals of Figs. 2i,j as $l\to 0$.

Appendix B: $O(\alpha_s)$ corrections from Fig. 4

We discuss the factorization of the initial-state collinear divergences in the $O(\alpha_s)$ radiative corrections to Fig. 1b, which are shown in Fig. 4. Inserting the Fierz identity, Fig. 1b gives only the lowest-order PS distribution amplitude $\phi_S^{(0)}$ and the hard amplitude $H_S^{(0)}$,

$$\phi_S^{(0)}(x_1,\xi_1) = \frac{1}{4m_0}\bar{d}(x_1P_1)\gamma_5 u(\bar{x}_1P_1)\delta(\xi_1-x_1),$$
$$H_S^{(0)}(\xi_1,x_2) = \frac{\mathrm{i}}{2}eg^2C_Fm_0 \qquad (B.1)$$
$$\times\frac{\mathrm{tr}[\gamma_\nu d(x_2P_2)\bar{u}(\bar{x}_2P_2)\gamma_\mu(\not{P}_1 - x_2\ \not{P}_2)\gamma^\nu\gamma^5]}{(P_1-x_2P_2)^2(\xi_1P_1-x_2P_2)^2},$$

because of $\gamma^\nu(\not{n}_+\ \not{n}_- - 1)\gamma_\nu = 0$, where the gamma matrices γ^ν and γ_ν come from the gluon vertices in Fig. 1b. The variable ξ_1 denotes a momentum fraction, which could be modified by collinear gluon exchanges.

The integral from Fig. 4b is written as

$$I^{(b)} = -\frac{1}{2}eg^4C_F^2\int\frac{\mathrm{d}^4l}{(2\pi)^4}\bar{d}(x_1P_1)\gamma_\beta\frac{x_1\ \not{P}_1 - \not{l}}{(x_1P_1-l)^2}$$
$$\times\gamma_\alpha\bar{d}(x_2P_2)u(\bar{x}_2P_2)$$
$$\times\gamma_\mu\frac{\not{P}_1 - x_2\ \not{P}_2}{(P_1-x_2P_2)^2}\gamma^\alpha\ \frac{\bar{x}_1\ \not{P}_1 + \not{l}}{(\bar{x}_1P_1+l)^2}\gamma^\beta u(\bar{x}_1P_1)$$
$$\times\frac{1}{l^2(x_2P_2-x_1P_1+l)^2}. \qquad (B.2)$$

Following the same procedure as for (A.1), we obtain

$$I^{(b)} \approx \int \mathrm{d}\xi_1\phi_{Sb}^{(1)}(x_1,\xi_1)H_S^{(0)}(\xi_1,x_2), \qquad (B.3)$$

where the expression of $\phi_{Sb}^{(1)}(x_1,\xi_1)$ has been given in (15). The factorization of Figs. 4a,c is performed in a similar way, leading to $\phi_{Sa,Sc}^{(1)}(x_1,\xi_1)$ in (14) and (16).

The loop integral associated with Fig. 4d is given by

$$I^{(d)} = \frac{\mathrm{i}eg^4}{2N_c}\int\frac{\mathrm{d}^4l}{(2\pi)^4}\bar{d}(x_1P_1)\gamma^\lambda d(x_2P_2)\bar{u}(\bar{x}_2P_2)$$
$$\times\gamma_\mu\frac{\not{P}_1 - x_2\ \not{P}_2}{(P_1-x_2P_2)^2}\gamma^\beta\frac{\bar{x}_1\ \not{P}_1 + \not{l}}{(\bar{x}_1P_1+l)^2} \qquad (B.4)$$
$$\times\gamma^\alpha u(\bar{x}_1P_1)\frac{\mathrm{tr}(T^cT^bT^a)\Gamma^{cba}_{\lambda\beta\alpha}}{l^2(x_1P_1-x_2P_2-l)^2(x_1P_1-x_2P_2)^2},$$

with the triple-gluon vertex in (A.4). The same procedure as for (A.3) leads to

$$I^{(d)} = eg^4\int\frac{\mathrm{d}^4l}{(2\pi)^4}\bar{d}(x_1P_1)\gamma_\beta\ d(x_2P_2)\bar{u}(\bar{x}_2P_2)\gamma_\mu$$
$$\times\frac{\not{P}_1 - x_2\ \not{P}_2}{(P_1-x_2P_2)^2}\gamma^\beta$$
$$\times\frac{\bar{x}_1\ \not{P}_1 + \not{l}}{(\bar{x}_1P_1+l)^2}\gamma_\alpha u(\bar{x}_1P_1)\frac{1}{l^2}\frac{n_{-\alpha}}{n_-\cdot l} \qquad (B.5)$$
$$\times\left[\frac{1}{(x_1P_1-x_2P_2)^2}-\frac{1}{(x_1P_1-x_2P_2-l)^2}\right].$$

Applying the eikonal approximation in (A.9) and the similar reasoning for Fig. 2g, the loop integrals associated with Figs. 4e,f,g are simplified into

$$I^{(e)}$$
$$= \frac{-eg^4C_F}{4N_c}\int\frac{\mathrm{d}^4l}{(2\pi)^4}\ \bar{d}(x_1P_1)\gamma^\alpha\ d(x_2P_2)\bar{u}(\bar{x}_2P_2)$$
$$\times\gamma_\mu\frac{\not{P}_1 - x_2\ \not{P}_2 + \not{l}}{(P_1-x_2P_2+l)^2}\gamma_\alpha \qquad (B.6)$$
$$\times\frac{\bar{x}_1\ \not{P}_1 + \not{l}}{(\bar{x}_1P_1+l)^2}\gamma^\beta u(\bar{x}_1P_1)\frac{1}{l^2}\frac{n_{-\beta}}{n_-\cdot l}\frac{1}{(x_1P_1-x_2P_2)^2},$$

$$
\begin{aligned}
&I^{(f)}\\
&= \frac{eg^4C_F}{4N_c}\int\frac{\mathrm{d}^4l}{(2\pi)^4}\,\bar{d}(x_1P_1)\gamma^\alpha\,d(x_2P_2)\bar{u}(\bar{x}_2P_2)\\
&\quad\times\gamma_\mu\frac{\not{P}_1-x_2\not{P}_2}{(P_1-x_2P_2)^2}\gamma_\alpha\\
&\quad\times\frac{\bar{x}_1\not{P}_1+\not{l}}{(\bar{x}_1P_1+l)^2}\gamma^\beta u(\bar{x}_1P_1)\frac{1}{l^2}\frac{n_{-\beta}}{n_-\cdot l}\frac{1}{(x_1P_1-x_2P_2-l)^2}\,,
\end{aligned}
\tag{B.7}
$$

$$
\begin{aligned}
&I^{(g)}\\
&= \frac{-eg^4C_F}{4N_c}\int\frac{\mathrm{d}^4l}{(2\pi)^4}\,\bar{d}(x_1P_1)\gamma^\alpha d(x_2P_2)\bar{u}(\bar{x}_2P_2)\\
&\quad\times\gamma_\mu\left(\frac{\not{P}_1-x_2\not{P}_2}{(P_1-x_2P_2)^2}-\frac{\not{P}_1-x_2\not{P}_2+\not{l}}{(P_1-x_2P_2+l)^2}\right)\\
&\quad\times\gamma_\alpha\,\frac{\bar{x}_1\not{P}_1+\not{l}}{(\bar{x}_1P_1+l)^2}\gamma^\beta u\,(\bar{x}_1P_1)\\
&\quad\times\frac{1}{l^2}\frac{n_{-\beta}}{n_-\cdot l}\frac{1}{(x_1P_1-x_2P_2)^2},
\end{aligned}
\tag{B.8}
$$

respectively. The integral $I^{(e)}$, in which the hard fermion propagator contains a residual dependence on l, is cancelled by the second term of $I^{(g)}$. It means that we can obtain the desired factorization formula, only after summing Figs. 4d–g. Inserting the Fierz identity, we have

$$
\sum_{i=(d)}^{(g)} I^i \approx \int \mathrm{d}\xi_1\phi^{(1)}_{\mathrm{S}u}(x_1,\xi_1)H^{(0)}_{\mathrm{S}}(\xi_1,x_2)\,,
\tag{B.9}
$$

with the functions $\phi^{(1)}_{\mathrm{S}u}$ and $H^{(0)}_{\mathrm{S}}$ given in (18) and (B.1), respectively.

The integral associated with Fig. 4h is given by

$$
\begin{aligned}
&I^{(h)}\\
&= \frac{-\mathrm{i}eg^4}{2N_c}\int\frac{\mathrm{d}^4l}{(2\pi)^4}\bar{d}(x_1P_1)\gamma^\lambda\frac{x_1\not{P}_1-\not{l}}{(x_1P_1-l)^2}\\
&\quad\times\gamma^\beta d(x_2P_2)\bar{u}(\bar{x}_2P_2)\gamma_\mu\frac{\not{P}_1-x_2\not{P}_2}{(P_1-x_2P_2)^2}\\
&\quad\times\gamma^\alpha u(\bar{x}_1P_1)\frac{\mathrm{tr}(T^cT^bT^a)\Gamma^{cba}_{\lambda\beta\alpha}}{l^2(x_1P_1-x_2P_2-l)^2(x_1P_1-x_2P_2)^2}\,,
\end{aligned}
\tag{B.10}
$$

with the triple-gluon vertex in (A.16). Following the same procedure as for Fig. 4d, the integral becomes

$$
\begin{aligned}
&I^{(h)}\\
&= -eg^4\int\frac{\mathrm{d}^4l}{(2\pi)^4}\bar{d}(x_1P_1)\gamma^\lambda\frac{x_1\not{P}_1-\not{l}}{(x_1P_1-l)^2}\\
&\quad\times\gamma_\alpha\beta d(x_2P_2)\bar{u}(\bar{x}_2P_2)\gamma_\mu\frac{\not{P}_1-x_2\not{P}_2}{(P_1-x_2P_2)^2}\gamma^\alpha\\
&\quad\times u(\bar{x}_1P_1)\frac{1}{l^2}\frac{n_{-\lambda}}{n_-\cdot l}\\
&\quad\times\left[\frac{1}{(x_1P_1-x_2P_2)^2}-\frac{1}{(x_1P_1-x_2P_2-l)^2}\right].
\end{aligned}
\tag{B.11}
$$

Similarly, we obtain

$$
\begin{aligned}
&I^{(i)}\\
&= \frac{eg^4C_F}{4N_c}\int\frac{\mathrm{d}^4l}{(2\pi)^4}\bar{d}(x_1P_1)\gamma^\alpha\frac{x_1\not{P}_1-\not{l}}{(x_1P_1-l)^2}\\
&\quad\times\gamma_\beta\beta d(x_2P_2)\bar{u}(\bar{x}_2P_2)\gamma_\mu\frac{\not{P}_1-x_2\not{P}_2}{(P_1-x_2P_2)^2}\\
&\quad\times\gamma^\beta u(\bar{x}_1P_1)\frac{1}{l^2}\frac{n_{-\alpha}}{n_-\cdot l}\frac{1}{(x_1P_1-x_2P_2)^2}\,,
\end{aligned}
\tag{B.12}
$$

$$
\begin{aligned}
&I^{(j)}\\
&= \frac{-eg^4C_F}{4N_c}\int\frac{\mathrm{d}^4l}{(2\pi)^4}\bar{d}(x_1P_1)\gamma^\alpha\frac{x_1\not{P}_1-\not{l}}{(x_1P_1-l)^2}\\
&\quad\times\gamma_\beta\beta d(x_2P_2)\bar{u}(\bar{x}_2P_2)\gamma_\mu\frac{\not{P}_1-x_2\not{P}_2-\not{l}}{(P_1-x_2P_2-l)^2}\\
&\quad\times\gamma^\beta u(\bar{x}_1P_1)\frac{1}{l^2}\frac{n_{-\alpha}}{n_-\cdot l}\frac{1}{(x_1P_1-x_2P_2-l)^2}\,,
\end{aligned}
\tag{B.13}
$$

$$
\begin{aligned}
&I^{(k)}\\
&= \frac{-eg^4C_F}{4N_c}\int\frac{\mathrm{d}^4l}{(2\pi)^4}\bar{d}(x_1P_1)\gamma^\alpha\frac{x_1\not{P}_1-\not{l}}{(x_1P_1-l)^2}\\
&\quad\times\gamma_\beta\beta d(x_2P_2)\bar{u}(\bar{x}_2P_2)\\
&\quad\times\gamma_\mu\left(\frac{\not{P}_1-x_2\not{P}_2}{(P_1-x_2P_2)^2}-\frac{\not{P}_1-x_2\not{P}_2-\not{l}}{(P_1-x_2P_2-l)^2}\right)\\
&\quad\times\gamma^\beta\,u(\bar{x}_1P_1)\frac{1}{l^2}\frac{n_{-\alpha}}{n_-\cdot l}\frac{1}{(x_1P_1-x_2P_2-l)^2}\,.
\end{aligned}
\tag{B.14}
$$

Combining (B.11)–(B.14) and inserting the Fierz identity, we derive

$$
\sum_{i=(h)}^{(k)} I^i \approx \int \mathrm{d}\xi_1\phi^{(1)}_{\mathrm{S}\bar{d}}(x_1,\xi_1)H^{(0)}_{\mathrm{S}}(\xi_1,x_2)\,,
\tag{B.15}
$$

with the collinear piece $\phi^{(1)}_{\mathrm{S}\bar{d}}$ shown in (20).

Appendix C: $O(\alpha_{\mathrm{s}})$ corrections to $B\to\pi\ell\nu$

In this appendix we demonstrate the collinear factorization of Fig. 4 for the semileptonic decay $B\to\pi l\nu$ with the initial and final states being flipped. As mentioned in Sec. 4, collinear divergences in this decay should be absorbed into the final-state pion. Figures 4a–c can be factorized straightforwardly, leading to (59).

The loop integral from Fig. 4d is given by

$$
\begin{aligned}
&I^{(d)}\\
&= \frac{-g^4}{2N_c}\int\frac{\mathrm{d}^4l}{(2\pi)^4}\bar{u}(\bar{x}_2P_2)\gamma^\beta\frac{\bar{x}_2\not{P}_2+\not{l}}{(\bar{x}_2P_2+l)^2}\\
&\quad\times\gamma^\alpha\frac{\not{P}_2-\not{k}_1}{(P_2-k_1)^2}\gamma_\mu b(P_1-k_1)\bar{d}(k_1)\\
&\quad\times\gamma^\lambda\bar{d}(x_2P_2)\frac{\mathrm{tr}(T^cT^bT^a)\Gamma^{cba}_{\lambda\beta\alpha}}{l^2(k_1-x_2P_2+l)^2(k_1-x_2P_2)^2}\,,
\end{aligned}
\tag{C.1}
$$

with the triple-gluon vertex,

$$\begin{aligned}\Gamma^{cba}_{\lambda\beta\alpha} = f^{cba}[&g_{\alpha\beta}(2l+k_1-x_2P_2)_\lambda \\ &+g_{\beta\lambda}(k_1-x_2P_2-l)_\alpha \\ &+g_{\lambda\alpha}(2x_2P_2-2k_1-l)_\beta]\,. \end{aligned} \tag{C.2}$$

The color factor is simplified according to (A.5). In the collinear region with l parallel to P_2, only the term proportional to $g_{\lambda\alpha}$ contributes a collinear divergence. The reason is as follows: due to the equations of motion for the two partons in the final-state pion, $\gamma^\beta = \gamma^-$ is favored, and γ^λ must be $\gamma_{\rm T}$. Because of $\gamma^\beta = \gamma^-$, only the plus component of k_1 in the third term on the right-hand side of (C.2) survives. We then apply the approximation similar to (A.6),

$$\begin{aligned}&\frac{2k_{1\beta}}{(k_1-x_2P_2)^2(k_1-x_2P_2+l)^2} \\ &\approx \frac{n_{+\beta}}{n_+\cdot l}\left[\frac{1}{(k_1-x_2P_2)^2}-\frac{1}{(k_1-x_2P_2+l)^2}\right],\end{aligned} \tag{C.3}$$

and (C.1) is simplified into

$$\begin{aligned}I^{(d)} &= {\rm i}g^4\int\frac{{\rm d}^4l}{(2\pi)^4}\bar u(\bar x_2P_2)\gamma^\beta\frac{\bar x_2\not P_2+\not l}{(\bar x_2P_2+l)^2} \\ &\quad\times\gamma^\alpha\frac{\not P_2-\not k_1}{(P_2-k_1)^2}\gamma_\mu b(P_1-k_1)\bar d(k_1)\gamma_\alpha \\ &\quad\times d(x_2P_2)\frac{1}{l^2}\frac{n_{+\beta}}{n_+\cdot l} \\ &\quad\times\left[\frac{1}{(k_1-x_2P_2)^2}-\frac{1}{(k_1-x_2P_2+l)^2}\right].\end{aligned} \tag{C.4}$$

The collinear factorization of Fig. 4e can be achieved by applying the eikonal approximation to the b quark propagator,

$$\begin{aligned}&\frac{\not P_1-\not k_1+\not l+m_b}{(P_1-k_1+l)^2-m_b^2}\gamma_\beta b(P_1-k_1) \\ &\approx\frac{2(P_1-k_1)_\beta-\gamma_\beta(\not P_1-\not k_1-m_b)}{2(P_1-k_1)\cdot l}b(P_1-k_1) \\ &\approx\frac{n_{+\beta}}{n_+\cdot l}b(P_1-k_1)\,.\end{aligned} \tag{C.5}$$

The neglect of $\not l$ is due to $\gamma_\beta=\gamma^+$ in the collinear region. The second term on the right-hand side of the first line vanishes because of (55). To derive the final expression, we have further dropped the power-suppressed terms proportional to k_1. The integral associated with Fig. 4e then becomes

$$\begin{aligned}I^{(e)} &= \frac{-{\rm i}g^4C_F}{4N_c}\int\frac{{\rm d}^4l}{(2\pi)^4}\bar u(\bar x_2P_2)\gamma^\beta\frac{\bar x_2\not P_2+\not l}{(\bar x_2P_2+l)^2} \\ &\quad\times\gamma^\alpha\frac{\not P_2-\not k_1+\not l}{(P_2-k_1+l)^2}\gamma_\mu b(P_1-k_1)\bar d(k_1)\gamma_\alpha \\ &\quad\times d(x_2P_2)\frac{1}{l^2}\frac{n_{+\beta}}{n_+\cdot l}\frac{1}{(k_1-x_2P_2)^2}\,.\end{aligned} \tag{C.6}$$

Similarly, for the integral of Fig. 4f the eikonal approximation

$$\begin{aligned}&\bar d(k_1)\gamma_\beta\frac{\not k_1+\not l}{(k_1+l)^2} \\ &\approx\bar d(k_1)\frac{2k_{1\beta}-\not k_1\gamma_\beta}{2k_1\cdot l}=\bar d(k_1)\frac{n_{+\beta}}{n_+\cdot l}\,,\end{aligned} \tag{C.7}$$

which stems from $\gamma_\beta=\gamma^+$ in the collinear region, leads to the simplified expression

$$\begin{aligned}I^{(f)} &= \frac{{\rm i}g^4C_F}{4N_c}\int\frac{{\rm d}^4l}{(2\pi)^4}\bar u(\bar x_2P_2)\gamma^\beta\frac{\bar x_2\not P_2+\not l}{(\bar x_2P_2+l)^2} \\ &\quad\times\gamma^\alpha\frac{\not P_2-\not k_1}{(P_2-k_1)^2}\gamma_\mu b(P_1-k_1)\bar d(k_1)\gamma_\alpha \\ &\quad\times d(x_2P_2)\frac{1}{l^2}\frac{n_{+\beta}}{n_+\cdot l}\frac{1}{(k_1-x_2P_2+l)^2}\,.\end{aligned} \tag{C.8}$$

The loop integral of Fig. 4g is written as

$$\begin{aligned}I^{(g)} &= \frac{-{\rm i}g^4C_F}{4N_c}\int\frac{{\rm d}^4l}{(2\pi)^4}\bar u(\bar x_2P_2)\gamma^\beta\frac{\bar x_2\not P_2+\not l}{(\bar x_2P_2+l)^2} \\ &\quad\times\gamma^\alpha\frac{\not P_2-\not k_1+\not l}{(P_2-k_1+l)^2}\gamma_\beta\frac{\not P_2-\not k_1}{(P_2-k_1)^2}\gamma_\mu b(P_1-k_1)\bar d(k_1) \\ &\quad\times\gamma_\alpha\; d(x_2P_2)\frac{1}{l^2(k_1-x_2P_2)^2}\,.\end{aligned} \tag{C.9}$$

In the collinear region with $l\parallel P_2$ we apply the decomposition similar to (A.12) because of $\gamma^\beta(\gamma_\beta)=\gamma^-(\gamma^+)$,

$$\begin{aligned}&\frac{\not P_2-\not k_1+\not l}{(P_2-k_1+l)^2}\gamma_\beta\frac{\not P_2-\not k_1}{(P_2-k_1)^2} \\ &=\frac{n_{+\beta}}{n_+\cdot l}\left[\frac{\not P_2-\not k_1}{(P_2-k_1)^2}-\frac{\not P_2-\not k_1+\not l}{(P_2-k_1+l)^2}\right],\end{aligned} \tag{C.10}$$

leading to

$$\begin{aligned}I^{(g)} &= \frac{-{\rm i}g^4C_F}{4N_c}\int\frac{{\rm d}^4l}{(2\pi)^4}\bar u(\bar x_2P_2)\gamma^\beta\frac{\bar x_2\not P_2+\not l}{(\bar x_2P_2+l)^2} \\ &\quad\times\gamma^\alpha\left(\frac{\not P_2-\not k_1}{(P_2-k_1)^2}-\frac{\not P_2-\not k_1+\not l}{(P_2-k_1+l)^2}\right) \\ &\quad\times\gamma_\mu b(P_1-k_1)\bar d(k_1)\gamma_\alpha\; d(x_2P_2)\frac{1}{l^2(k_1-x_2P_2)^2}\,.\end{aligned} \tag{C.11}$$

The sum of (C.4), (C.6), (C.8) and (C.11) gives

$$\sum_{i=(d)}^{(g)} I^i$$

$$= \frac{\mathrm{i}g^4 C_F^2}{2} \int \frac{\mathrm{d}^4 l}{(2\pi)^4} \bar{u}(\bar{x}_2 P_2)\gamma^\beta \frac{\bar{x}_2 \not{P}_2 + \not{l}}{(\bar{x}_2 P_2 + l)^2} \times\gamma^\alpha \frac{\not{P}_2 - \not{k}_1}{(P_2 - k_1)^2}\gamma_\mu b(P_1 - k_1)\bar{d}(k_1)\gamma_\alpha \times d(x_2 P_2)\frac{1}{l^2}\frac{n_+\beta}{n_+ \cdot l} \times \left[\frac{1}{(k_1 - x_2 P_2)^2} - \frac{1}{(k_1 - x_2 P_2 + l)^2}\right] . \quad \text{(C.12)}$$

Inserting the Fierz identity, we obtain the desired collinear factorization in (63) with the hard amplitude $H_{\mathrm{S}}^{(0)}$ in (58) and the collinear piece $\phi_{\mathrm{S}u}^{(1)}$ in (64). The above result is consistent with that expected from the Ward identity.

For Figs. 4h–k associated with the collinear gluon emitted from the outgoing $\bar{d}$ quark, the collinear factorization can be performed in an analogous way. The loop integral from Fig. 4h is written as

$$I^{(h)} = \frac{g^4}{2N_c} \int \frac{\mathrm{d}^4 l}{(2\pi)^4} \bar{u}(\bar{x}_2 P_2)\gamma^\alpha \frac{\not{P}_2 - \not{k}_1}{(P_2 - k_1)^2} \times\gamma_\mu b(P_1 - k_1)\bar{d}(k_1)\gamma^\lambda \frac{x_2 \not{P}_2 - \not{l}}{(x_2 P_2 - l)^2} \times\gamma^\beta\, d(x_2 P_2) \frac{\mathrm{tr}(T^c T^b T^a)\Gamma^{cba}_{\lambda\beta\alpha}}{l^2 (k_1 - x_2 P_2 + l)^2 (k_1 - x_2 P_2)^2} , \quad \text{(C.13)}$$

with the triple-gluon vertex,

$$\Gamma^{cba}_{\lambda\beta\alpha} = f^{cba}[g_{\beta\lambda}(2l + k_1 - x_2 P_2)_\alpha + g_{\alpha\beta}(k_1 - x_2 P_2 - l)_\lambda + g_{\lambda\alpha}(2x_2 P_2 - 2k_1 - l)_\beta] . \quad \text{(C.14)}$$

Following the same procedure as for Fig. 4d, (C.13) reduces to

$$I^{(h)} = -\mathrm{i}g^4 \int \frac{\mathrm{d}^4 l}{(2\pi)^4} \bar{u}(\bar{x}_2 P_2)\gamma^\alpha \frac{\not{P}_2 - \not{k}_1}{(P_2 - k_1)^2} \times\gamma_\mu b(P_1 - k_1)\bar{d}(k_1)\gamma_\alpha \times \frac{x_2 \not{P}_2 - \not{l}}{(x_2 P_2 - l)^2}\gamma^\beta\, d(x_2 P_2)\frac{1}{l^2}\frac{n_+\beta}{n_+ \cdot l} \times \left[\frac{1}{(k_1 - x_2 P_2)^2} - \frac{1}{(k_1 - x_2 P_2 + l)^2}\right] . \quad \text{(C.15)}$$

The loop integrals associated with Figs. 4i,j are given by

$$I^{(i)} = \frac{-\mathrm{i}g^4 C_F}{4N_c} \int \frac{\mathrm{d}^4 l}{(2\pi)^4} \bar{u}(\bar{x}_2 P_2)\gamma^\alpha \frac{\not{P}_2 - \not{k}_1}{(P_2 - k_1)^2} \times\gamma_\mu b(P_1 - k_1)\bar{d}(k_1)\gamma_\beta \frac{\not{k}_1 - \not{l}}{(k_1 - l)^2}\gamma_\alpha \times \frac{x_2 \not{P}_2 - \not{l}}{(x_2 P_2 - l)^2}\gamma^\beta \bar{d}(x_2 P_2)\frac{1}{l^2 (k_1 - x_2 P_2)^2} , \quad \text{(C.16)}$$

$$I^{(j)} = \frac{\mathrm{i}g^4 C_F}{4N_c} \int \frac{\mathrm{d}^4 l}{(2\pi)^4} \bar{u}(\bar{x}_2 P_2)\gamma^\alpha \frac{\not{P}_2 - \not{k}_1 - \not{l}}{(P_2 - k_1 - l)^2} \times\gamma_\mu \frac{\not{P}_1 - \not{k}_1 - \not{l} + m_b}{(P_1 - k_1 - l)^2 - m_b^2}\gamma_\beta b(P_1 - k_1) \times \bar{d}(k_1)\gamma_\alpha \frac{x_2 \not{P}_2 - \not{l}}{(x_2 P_2 - l)^2}\gamma^\beta \bar{d}(x_2 P_2)\frac{1}{l^2 (k_1 - x_2 P_2 + l)^2} . \quad \text{(C.17)}$$

Using the approximations similar to (C.5) and (C.7), the above expressions are simplified into

$$I^{(i)} = \frac{\mathrm{i}g^4 C_F}{4N_c} \int \frac{\mathrm{d}^4 l}{(2\pi)^4} \bar{u}(\bar{x}_2 P_2)\gamma^\alpha \frac{\not{P}_2 - \not{k}_1}{(P_2 - k_1)^2} \times\gamma_\mu b(P_1 - k_1)\bar{d}(k_1)\gamma_\alpha \times \frac{x_2 \not{P}_2 - \not{l}}{(x_2 P_2 - l)^2}\gamma^\beta \bar{d}(x_2 P_2)\frac{1}{l^2}\frac{n_+\beta}{n_+ \cdot l}\frac{1}{(k_1 - x_2 P_2)^2} , \quad \text{(C.18)}$$

$$I^{(j)} = \frac{-\mathrm{i}g^4 C_F}{4N_c} \int \frac{\mathrm{d}^4 l}{(2\pi)^4} \bar{u}(\bar{x}_2 P_2)\gamma^\alpha \frac{\not{P}_2 - \not{k}_1 - \not{l}}{(P_2 - k_1 - l)^2} \times\gamma_\mu b(P_1 - k_1)\bar{d}(k_1)\gamma_\alpha \times \frac{x_2 \not{P}_2 - \not{l}}{(x_2 P_2 - l)^2}\gamma^\beta \bar{d}(x_2 P_2)\frac{1}{l^2}\frac{n_+\beta}{n_+ \cdot l}\frac{1}{(k_1 - x_2 P_2 + l)^2} . \quad \text{(C.19)}$$

We then consider the loop integral from Fig. 4k, which is given by

$$I^{(k)} = \frac{\mathrm{i}g^4 C_F}{4N_c} \int \frac{\mathrm{d}^4 l}{(2\pi)^4} \bar{u}(\bar{x}_2 P_2)\gamma^\alpha \frac{\not{P}_2 - \not{k}_1 - \not{l}}{(P_2 - k_1 - l)^2} \times\gamma_\beta \frac{\not{P}_2 - \not{k}_1}{(P_2 - k_1)^2}\gamma_\mu b(P_1 - k_1)\bar{d}(k_1) \times\gamma_\alpha \frac{x_2 \not{P}_2 - \not{l}}{(x_2 P_2 - l)^2}\gamma^\beta \bar{d}(x_2 P_2)\frac{1}{l^2 (k_1 - x_2 P_2 + l)^2} . \quad \text{(C.20)}$$

With the reasoning applied to Fig. 4g, the above expression becomes

$$I^{(k)} = \frac{-\mathrm{i}g^4 C_F}{4N_c} \int \frac{\mathrm{d}^4 l}{(2\pi)^4} \bar{u}(\bar{x}_2 P_2)(I)_{ij} \times\gamma^\alpha \left(\frac{\not{P}_2 - \not{k}_1}{(P_2 - k_1)^2} - \frac{\not{P}_2 - \not{k}_1 - \not{l}}{(P_2 - k_1 - l)^2}\right)\gamma_\mu b(P_1 - k_1) \times \bar{d}(k_1)\gamma_\alpha \frac{x_2 \not{P}_2 - \not{l}}{(x_2 P_2 - l)^2}\gamma^\beta\, d(x_2 P_2) \times \frac{1}{l^2}\frac{n_+\beta}{n_+ \cdot l}\frac{1}{(k_1 - x_2 P_2 + l)^2} . \quad \text{(C.21)}$$

The sum of Figs. 4h–k gives

$$\begin{aligned}
&\sum_{i=(h)}^{(k)} I^i \\
&= \frac{-\mathrm{i}g^4 C_F^2}{2}\int\frac{\mathrm{d}^4 l}{(2\pi)^4}\bar{u}(\bar{x}_2P_2)\gamma^\alpha\frac{\not{P}_2-\not{k}_1}{(P_2-k_1)^2} \\
&\quad\times\gamma_\mu b(P_1-k_1)\bar{d}(k_1)\gamma_\alpha \\
&\quad\times\frac{x_2\not{P}_2-\not{l}}{(x_2P_2-l)^2}\gamma^\beta\, d(x_2P_2)\frac{1}{l^2}\frac{n_{+\beta}}{n_+\cdot l} \\
&\quad\times\left[\frac{1}{(k_1-x_2P_2)^2}-\frac{1}{(k_1-x_2P_2+l)^2}\right], \qquad \text{(C.22)}
\end{aligned}$$

from which we obtain (65).

We then discuss the factorization of the collinear divergences from Fig. 2 with the initial and final states being flipped, which represents the $O(\alpha_s)$ corrections to Fig. 1b. To simplify the discussion, we show only the PS parts below. For the irreducible diagrams associated with the collinear gluon emitted from the outgoing u quark, the results are

$$\begin{aligned}
&I^{(d)} \\
&= \mathrm{i}g^4\int\frac{\mathrm{d}^4 l}{(2\pi)^4}\bar{u}(\bar{x}_2P_2)\gamma^\beta\frac{\bar{x}_2\not{P}_2+\not{l}}{(\bar{x}_2P_2+l)^2}(I)_{ij} \\
&\quad\times\gamma_\mu\frac{\not{P}_1-x_2\not{P}_2+\not{l}+m_b}{(P_1-x_2P_2+l)^2-m_b^2}\gamma^\alpha b(P_1-k_1)\bar{d}(k_1)\gamma_\alpha \\
&\quad\times d(x_2P_2)\,\frac{1}{l^2}\frac{n_{+\beta}}{n_+\cdot l} \\
&\quad\times\left[\frac{1}{(k_1-x_2P_2)^2}-\frac{1}{(k_1-x_2P_2+l)^2}\right], \qquad \text{(C.23)}
\end{aligned}$$

$$\begin{aligned}
&I^{(e)} \\
&= \frac{-\mathrm{i}g^4 C_F}{4N_c}\int\frac{\mathrm{d}^4 l}{(2\pi)^4}\bar{u}(\bar{x}_2P_2)\gamma^\beta\frac{\bar{x}_2\not{P}_2+\not{l}}{(\bar{x}_2P_2+l)^2} \\
&\quad\times\gamma_\mu\frac{\not{P}_1-x_2\not{P}_2+\not{l}+m_b}{(P_1-x_2P_2+l)^2-m_b^2}\gamma^\alpha b(P_1-k_1) \\
&\quad\times\bar{d}(k_1)\gamma_\alpha\, d(x_2P_2)\,\frac{1}{l^2}\frac{n_{+\beta}}{n_+\cdot l}\frac{1}{(k_1-x_2P_2)^2}, \qquad \text{(C.24)}
\end{aligned}$$

$$\begin{aligned}
&I^{(f)} \\
&= \frac{\mathrm{i}g^4 C_F}{4N_c}\int\frac{\mathrm{d}^4 l}{(2\pi)^4}\bar{u}(\bar{x}_2P_2)\gamma^\beta\frac{\bar{x}_2\not{P}_2+\not{l}}{(\bar{x}_2P_2+l)^2} \\
&\quad\times\gamma_\mu\frac{\not{P}_1-x_2\not{P}_2+\not{l}+m_b}{(P_1-x_2P_2+l)^2-m_b^2}\gamma^\alpha b(P_1-k_1) \\
&\quad\times\bar{d}(k_1)\gamma_\alpha\, d(x_2P_2)\,\frac{1}{l^2}\frac{n_{+\beta}}{n_+\cdot l}\frac{1}{(k_1-x_2P_2+l)^2}, \qquad \text{(C.25)}
\end{aligned}$$

$$\begin{aligned}
&I^{(g)} \\
&= \frac{\mathrm{i}g^4 C_F^2}{2}\int\frac{\mathrm{d}^4 l}{(2\pi)^4}\bar{u}(\bar{x}_2P_2)\gamma^\beta\frac{\bar{x}_2\not{P}_2+\not{l}}{(\bar{x}_2P_2+l)^2} \\
&\quad\times\gamma_\mu\left(\frac{\not{P}_1-x_2\not{P}_2+m_b}{(P_1-x_2P_2)^2-m_b^2}-\frac{\not{P}_1-x_2\not{P}_2+\not{l}+m_b}{(P_1-x_2P_2+l)^2-m_b^2}\right) \\
&\quad\times\gamma^\alpha b(P_1-k_1)\bar{d}(k_1)\gamma_\alpha\, d(x_2P_2) \\
&\quad\times\frac{1}{l^2}\frac{n_{+\beta}}{n_+\cdot l}\frac{1}{(k_1-x_2P_2)^2}. \qquad \text{(C.26)}
\end{aligned}$$

The combination of Figs. 2d–g separates into two terms,

$$\begin{aligned}
&\sum_{i=(d)}^{(g)} I^i \\
&= \frac{\mathrm{i}g^4 C_F^2}{2}\int\frac{\mathrm{d}^4 l}{(2\pi)^4}\bar{u}(\bar{x}_2P_2)\gamma^\beta\frac{\bar{x}_2\not{P}_2+\not{l}}{(\bar{x}_2P_2+l)^2} \\
&\quad\times\gamma_\mu\frac{\not{P}_1-x_2\not{P}_2+m_b}{(P_1-x_2P_2)^2-m_b^2}\gamma^\alpha \\
&\quad\times b(P_1-k_1)\bar{d}(k_1)\gamma_\alpha\, d(x_2P_2)\,\frac{1}{l^2}\frac{n_{+\beta}}{n_+\cdot l}\frac{1}{(k_1-x_2P_2)^2} \\
&\quad-\frac{\mathrm{i}g^4 C_F^2}{2}\int\frac{\mathrm{d}^4 l}{(2\pi)^4}\bar{u}(\bar{x}_2P_2)\gamma^\beta\frac{\bar{x}_2\not{P}_2+\not{l}}{(\bar{x}_2P_2+l)^2} \\
&\quad\times\gamma_\mu\frac{\not{P}_1-x_2\not{P}_2+\not{l}+m_b}{(P_1-x_2P_2+l)^2-m_b^2}\gamma^\alpha \\
&\quad\times b(P_1-k_1)\bar{d}(k_1)\gamma_\alpha\, d(x_2P_2) \\
&\quad\times\frac{1}{l^2}\frac{n_{+\beta}}{n_+\cdot l}\frac{1}{(k_1-x_2P_2+l)^2}, \qquad \text{(C.27)}
\end{aligned}$$

from which we arrive at (72) after inserting the Fierz identity.

Similarly, we obtain the simplified expressions for the loop integrals from Figs. 2h–k,

$$\begin{aligned}
&I^{(h)} \\
&= -\mathrm{i}g^4\int\frac{\mathrm{d}^4 l}{(2\pi)^4}\bar{u}(\bar{x}_2P_2)\gamma_\mu\frac{\not{P}_1-x_2\not{P}_2+m_b}{(P_1-x_2P_2)^2-m_b^2} \\
&\quad\times\gamma^\alpha b(P_1-k_1)\bar{d}(k_1)\gamma_\alpha \\
&\quad\times\frac{x_2\not{P}_2-\not{l}}{(x_2P_2-l)^2}\gamma^\beta\, d(x_2P_2)\frac{1}{l^2}\frac{n_{+\beta}}{n_+\cdot l} \\
&\quad\times\left[\frac{1}{(k_1-x_2P_2)^2}-\frac{1}{(k_1-x_2P_2+l)^2}\right], \qquad \text{(C.28)}
\end{aligned}$$

$$\begin{aligned}
&I^{(i)} \\
&= \frac{\mathrm{i}g^4 C_F}{4N_c}\int\frac{\mathrm{d}^4 l}{(2\pi)^4}\bar{u}(\bar{x}_2P_2)\gamma_\mu\frac{(\not{P}_1-x_2\not{P}_2+m_b)}{(P_1-x_2P_2)^2-m_b^2} \\
&\quad\times\gamma^\alpha b(P_1-k_1)\bar{d}(k_1)\gamma_\alpha \qquad \text{(C.29)} \\
&\quad\times\frac{x_2\not{P}_2-\not{l}}{(x_2P_2-l)^2}\gamma^\beta\, d(x_2P_2)\frac{1}{l^2}\frac{n_{+\beta}}{n_+\cdot l}\frac{1}{(k_1-x_2P_2)^2}, \\
&I^{(j)} \\
&= \frac{-\mathrm{i}g^4 C_F}{4N_c}\int\frac{\mathrm{d}^4 l}{(2\pi)^4}\bar{u}(\bar{x}_2P_2)\gamma_\mu\frac{\not{P}_1-x_2\not{P}_2+m_b}{(P_1-x_2P_2)^2-m_b^2} \\
&\quad\times\gamma^\alpha b(P_1-k_1)\bar{d}(k_1)\gamma_\alpha \qquad \text{(C.30)} \\
&\quad\times\frac{x_2\not{P}_2-\not{l}}{(x_2P_2-l)^2}\gamma^\beta\, d(x_2P_2)\frac{1}{l^2}\frac{n_{+\beta}}{n_+\cdot l}\frac{1}{(k_1-x_2P_2+l)^2},
\end{aligned}$$

$$
\begin{aligned}
&I^{(k)}\\
&= \frac{-\mathrm{i}g^4C_F^2}{2}\int\frac{\mathrm{d}^4l}{(2\pi)^4}\bar{u}(\bar{x}_2P_2)\\
&\quad\times\gamma_\mu\left(\frac{\not P_1-x_2\not P_2+m_b}{(P_1-x_2P_2)^2-m_b^2}-\frac{\not P_1-x_2\not P_2+\not l+m_b}{(P_1-x_2P_2+l)^2-m_b^2}\right)\\
&\quad\times\gamma^\alpha b(P_1-k_1)\bar{d}(k_1)\gamma_\alpha\frac{x_2\not P_2-\not l}{(x_2P_2-l)^2}\gamma^\beta\, d(x_2P_2)\\
&\quad\times\frac{1}{l^2}\frac{n_{+\beta}}{n_+\cdot l}\frac{1}{(k_1-x_2P_2+l)^2}\,. \qquad \text{(C.31)}
\end{aligned}
$$

The combination of Figs. 2h–k separates into two terms:

$$
\begin{aligned}
&I^{(k)}\\
&= \frac{-\mathrm{i}g^4C_F^2}{2}\int\frac{\mathrm{d}^4l}{(2\pi)^4}\bar{u}(\bar{x}_2P_2)\gamma_\mu\frac{\not P_1-x_2\not P_2+m_b}{(P_1-x_2P_2)^2-m_b^2}\\
&\quad\times\gamma^\alpha b(P_1-k_1)\bar{d}(k_1)\gamma_\alpha\\
&\quad\times\frac{x_2\not P_2-\not l}{(x_2P_2-l)^2}\gamma^\beta\, d(x_2P_2)\frac{1}{l^2}\frac{n_{+\beta}}{n_+\cdot l}\frac{1}{(k_1-x_2P_2)^2}\\
&\quad-\frac{-\mathrm{i}g^4C_F^2}{2}\int\frac{\mathrm{d}^4l}{(2\pi)^4}\bar{u}(\bar{x}_2P_2)\gamma_\mu\frac{\not P_1-x_2\not P_2+\not l+m_b}{(P_1-x_2P_2+l)^2-m_b^2}\\
&\quad\times\gamma^\alpha b(P_1-k_1)\bar{d}(k_1)\gamma_\alpha \qquad \text{(C.32)}\\
&\quad\times\frac{x_2\not P_2-\not l}{(x_2P_2-l)^2}\gamma^\beta\, d(x_2P_2)\frac{1}{l^2}\frac{n_{+\beta}}{n_+\cdot l}\frac{1}{(k_1-x_2P_2+l)^2}\,,
\end{aligned}
$$

from which we arrive at (73) after inserting the Fierz identity.

References

1. H-n. Li, Phys. Rev. D **64**, 014019 (2001)
2. S.J. Brodsky, G.P. Lepage, Phys. Lett. B 87, 359 (1979); Phys. Rev. Lett. **43**, 545 (1979); G.P. Lepage, S. Brodsky, Phys. Rev. D **22**, 2157 (1980)
3. S.J. Brodsky, Y. Frishman, G.P. Lepage, C. Sachrajda, Phys. Lett. B **91**, 239 (1980)
4. A.V. Efremov, A.V. Radyushkin, Theor. Math. Phys. **42**, 97 (1980); Phys. Lett. B **94**, 245 (1980); I.V. Musatov, A.V. Radyushkin, Phys. Rev. D **56**, 2713 (1997)
5. A. Duncan, A.H. Mueller, Phys. Lett. B **90**, 159 (1980); Phys. Rev. D **21**, 1636 (1980)
6. V.L. Chernyak, A.R. Zhitnitsky, V.G. Serbo, JETP Lett. **26**, 594 (1977)
7. H-n. Li, 89-93, Proceedings for 4th International Conference on B Physics and CP Violation (BCP4), Japan, 2001, 360–364, Proceedings for 5th KEK Topical Conference: Frontiers in Flavor Physics (KEKTC5), Japan, 2001
8. C.H. Chen, Y.Y. Keum, H-n. Li, Phys. Rev. D **64**, 112002 (2001)
9. V.M. Braun, I.E. Filyanov, Z. Phys. C **48**, 239 (1990); P. Ball, J. High Energy Phys. **01**, 010 (1999)
10. B.V. Geshkenbein, M.V. Terentev, Phys. Lett. B **117**, 243 (1982); T.W. Yeh, Phys. Rev. D **65**, 074016 (2002); F.G. Cao, Y.B. Dai, C.S. Huang, Eur. Phys. J. C **11**, 501 (1999) and references therein
11. G.P. Korchemsky, D. Pirjol, T.M. Yan, Phys. Rev. D **61**, 114510 (2000)
12. E. Lunghi, D. Pirjol, D. Wyler, Nucl. Phys. B **649**, 349 (2003)
13. S. Descotes, C.T. Sachrajda, Nucl. Phys. B **625**, 239 (2002)
14. A. Szczepaniak, E.M. Henley, S. Brodsky, Phys. Lett. B **243**, 287 (1990)
15. G. Burdman, J.F. Donoghue, Phys. Lett. B **270**, 55 (1991)
16. M. Beneke, T. Feldmann, Nucl. Phys. B **592**, 3 (2000)
17. J. Botts, G. Sterman, Nucl. Phys. B **225**, 62 (1989)
18. H-n. Li, G. Sterman, Nucl. Phys. B **381**, 129 (1992)
19. M. Nagashima, H-n. Li, Phys. Rev. D **67**, 034001 (2003)
20. R. Ahkoury, G. Sterman, Y.P. Yao, Phys. Rev. D **50**, 358 (1994)
21. H-n. Li, Phys. Rev. D **66**, 094010 (2002)
22. S. Descotes-Genon, C.T. Sachrajda, Nucl. Phys. B **650**, 356 (2003)
23. H-n. Li, Phys. Rev. D **55**, 105 (1997); Phys. Lett. B **454**, 328 (1999); Chin. J. Phys. **37**, 569 (1999)
24. T. Kurimoto, H-n. Li, A.I. Sanda, Phys. Rev. D **65**, 014007 (2002)
25. M. Beneke, G. Buchalla, M. Neubert, C.T. Sachrajda, Phys. Rev. Lett. **83**, 1914 (1999); Nucl. Phys. B **591**, 313 (2000); B **606**, 245 (2001)
26. C.W. Bauer, S. Fleming, M. Luke, Phys. Rev. D **63**, 014006 (2001)
27. C.W. Bauer, S. Fleming, D. Pirjol, I.W. Stewart, Phys. Rev. D **63**, 114020 (2001)
28. C.W. Bauer, D. Pirjol, I.W. Stewart, Phys. Rev. Lett. **87**, 201806 (2001)
29. H-n. Li, Czech. J. Phys. **53**, 657 (2003); Prog. Part. Nucl. Phys. **51**, 85 (2003)
30. Z.T. Wei, M.Z. Yang, Nucl. Phys. B **642**, 263 (2002)
31. H-n. Li, H.S. Liao, hep-ph/0404050
32. C.W. Bauer, D. Pirjol, I.W. Stewart, Phys. Rev. D **67**, 071502 (2003)
33. H-n. Li, hep-ph/0304217
34. Y.Y. Keum, H-n. Li, A.I. Sanda, AIP Conf. Proc. **618**, 229 (2002); Y.Y. Keum, A.I. Sanda, Phys. Rev. D **67**, 054009 (2003)
35. C. Becchi, A. Rouet, R. Stora, Phys. Lett. B **52**, 344 (1974)
36. A.G. Grozin, M. Neubert, Phys. Rev. D **55**, 272 (1997)
37. A. Khodjamirian et al., Phys. Lett. B **410**, 275 (1997)
38. H-n. Li, H.L. Yu, Phys. Rev. Lett. **74**, 4388 (1995); Phys. Lett. B **353**, 301 (1995); Phys. Rev. D **53**, 2480 (1996)
39. Y.Y. Keum, H-n. Li, A.I. Sanda, Phys. Lett. B **504**, 6 (2001); Phys. Rev. D **63**, 054008 (2001); Y.Y. Keum, H-n. Li, Phys. Rev. D **63**, 074006 (2001)
40. C.D. Lu, K. Ukai, M.Z. Yang, Phys. Rev. D **63**, 074009 (2001)
41. C.H. Chang, H-n. Li, Phys. Rev. D **55**, 5577 (1997)
42. T.W. Yeh, H-n. Li, Phys. Rev. D **56**, 1615 (1997)